UTILIZING ZEBRAFISH TO MODEL THE CHILDHOOD BLINDING DISORDER, FAMILIAL EXUDATIVE VITREORETINOPATHY (FEVR), AND DISCOVER NOVEL THERAPEUTICS

By

Tenille R. Fleischhacker

Submitted in partial fulfillment of the requirements
for the degree of Master of Science

at
Dalhousie University
Halifax, Nova Scotia
August 2016

TABLE OF CONTENTS

LIST OF TABLES ..... **...v**

LIST OF FIGURES ..... **vii**

ABSTRACT ..... **viiii**

LIST OF ABBREVIATIONS & SYMBOLS USED ..... **ixx**

ACKNOWLEDGEMENTS ..... **xii**

CHAPTER 1: INTRODUCTION **1**

1.1 Human retinal development 1

1.2 Familial exudative vitreoretinopathy (FEVR) 6

1.3 Genetic etiology of FEVR 13

1.4 *CDH5*- a novel FEVR gene 17

1.5 Sphingosine-1-phosphate (S1P) receptors and JTE-013 19

1.6 Zebrafish as a preclinical FEVR model 24

1.7 Zebrafish retinal development 24

1.8 Zebrafish gene manipulation to create mutants and morphants 28

1.9 Drug screens utilizing zebrafish 31

1.10 Hypothesis and rationale 32

CHAPTER 2: MATERIALS & METHODS **33**

2.1 Zebrafish husbandry and housing 33

2.2 Morpholino oligonucleotide (MO) 34

2.3 Zebrafish imaging 35

2.4 Toxicity curves 35

2.5 Preliminary drug screen 36

2.6 Qualitative retinal vascular scale 39

2.7 Zebrafish *fzd4*$^{-/-}$ transgenic line construction & genotyping 41

2.8 *fzd4* $^{-/-}$ eye size analyses 41

2.9 *fzd4* $^{-/-}$ retinal whole mounts 42

2.10 Statistical analyses 43

CHAPTER 3: RESULTS 44

3.1 *cdh5* morphants display a robust decrease in retinal vasculature 44

3.2 Toxicity curves and MTD 46

3.3 Preliminary drug screen shows JTE-013 & compound 1 significantly affect "area inner eye" 52

3.4 Qualitative retinal vascular scale shows an improvement in "area inner eye" is associated with improved retinal vasculature 57

3.5 *fzd4*$^{-/-}$ mutants show no difference in eye size 59

3.6 *fzd4*$^{-/-}$ retinal whole mounts are difficult to interpret 62

CHAPTER 4: DISCUSSION 65

4.1 Summary 65

4.2 *cdh5* morphants display a FEVR-like phenotype……67

4.3 Eye size can potentially be used as a surrogate of retinal vascular disease 67

4.4 S1PR2 can successfully be targeted in *cdh5* morphant zebrafish……...69

4.5 *fzd4*$^{-/-}$ mutant zebrafish do not possess an obvious early larval phenotype……..…72

4.6 Potential significance for other retinal vascular disorders……...73

4.7 Limitations 75

4.8 Future directions……..76

4.9 Conclusions 77

REFERENCES 79

APPENDIX A COPYRIGHT AND PERMISSIONS- *PROGRESS IN RETINAL EYE RESEARCH* (ELSEVIER)……90

APPENDIX B COPYRIGHT AND PERMISSIONS- *OPHTHALMIC GENETICS* (TAYLOR AND FRANCIS)……...91

APPENDIX C COPYRIGHT AND PERMISSIONS- *INVESTIGATIVE OPHTHALMOLOGY AND VISUAL SCIENCE* (ASSOCIATION FOR RESEARCH IN VISION AND OPHTHALMOLOGY)…….…....92

APPENDIX D COPYRIGHT AND PERMISSIONS- *CELL* (ELSEVIER)……..…93

APPENDIX E COPYRIGHT AND PERMISSIONS- *AMERICAN JOURNAL OF CANCER RESEARCH* (E-CENTURY PUBLISHING CORPORATION)…..……..94

APPENDIX F COPYRIGHT AND PERMISSIONS- *DEVELOPMENTAL DYNAMICS* (JOHN WILEY AND SONS)……....95

APPENDIX G- ETHICS…….96

LIST OF TABLES

Table 1.1. Clinical staging of FEVR. 12
Table 1.2. Molecular modeling of S1PR2 binding pocket predicted this list of S1PR2 antagonists. 23
Table 1.3. Zebrafish and human retina share several similarities and differences. 26

LIST OF FIGURES

Figure 1.1. Human retinal vasculature emerges from the optic disc to periphery during development. 5
Figure 1.2. Comparison between normal retina and severe FEVR phenotype. 9
Figure 1.3. Strabismus in severley affected FEVR patient. 10
Figure 1.4. FEVR genes play a role in the canonical Wnt pathway. 16
Figure 1.5. S1PR2 inhibits vascular development while S1PR1 and S1PR3 promote vessel growth. 20
Figure 1.6. WT zebrafish eye histology and vascular anatomy. 27
Figure 1.7. Retinal whole mounts in adult *fzd4* mutant zebrafish display a FEVR-like phenotype. 30
Figure 2.1. Zebrafish eyes at 4 dpf displaying the six parameters used to measure eye size. 38
Figure 2.2. Representative images used in a qualitative retinal vascular scale. 40
Figure 3.1. Zebrafish injected with *cdh5* MO at the one cell stage display a robust decrease in retinal vasculature 45
Figure 3.2. Toxicity curve for JTE-013 with an MTD of 12.5 μM. 48
Figure 3.3. Toxicity curve for compound 1 with an MTD of 10 μM. 48
Figure 3.4. Toxicity curve for compound 2 with an MTD of 15 μM. 49
Figure 3.5. Toxicity curve for compound 3 with an MTD of 10 μM. 50
Figure 3.6. Toxicity curve for compound 4 with an MTD of 20 μM. 51
Figure 3.7. JTE-013 significantly improves “area inner eye” in *cdh5* morphants in a dose dependent manner. 54
Figure 3.8. Compound 1 significantly affects “area inner eye” in *cdh5* morphants. 55
Figure 3.9. Compound 2 has no effect on eye size in *cdh5* morphants. 56
Figure 3.10. Retinal vasculature appears to be associated with improvements in “area inner eye”. 58
Figure 3.11. WT and *fzd4*$^{-/-}$ *Tg*(*fli1a*:*EGFP)* zebrafish display organized retinal and tail vasculature at 4 dpf. 60
Figure 3.12. Eye size is not significantly different between WT and *fzd4*$^{-/-}$ *Tg*(*fli1a*:*EGFP)* zebrafish at 4dpf. 61

Figure 3.13. Representative images of one month old zebrafish retinal whole mounts are difficult to interpret. 64
Figure 3.14. Adult *fzd4*$^{-/-}$ zebrafish retinal whole mounts at three months following JTE-013 treatment do not show any obvious signs of improvement. 65

ABSTRACT

Familial exudative vitreoretinopathy (FEVR) is a blinding disorder that results in incomplete peripheral retinal vascularization at birth and there is currently no treatment. Zebrafish were used as a model to mimic a FEVR-like phenotype in order to carry out a preliminary drug screen for novel therapeutic compounds. A novel FEVR gene, *cdh5*, was knocked down using morpholino oligonucleotide and displayed a robust retinal phenotype and smaller eye size. Sphinghosine-1 phosphate receptor-2 (S1PR2) is a known inhibitor of blood vessel development. Several compounds predicted to interact with S1PR2 were screened using the *cdh5* morphant zebrafish including an S1PR2 inhibitor; JTE-013. JTE-013 significantly improved eye size establishing that S1PR2 can be targeted in zebrafish. "Compound 1" significantly decreased eye size, whereas "compound 2" had no effect. Thus, S1PR2 is a possible pharmacological target for the treatment of FEVR.

LIST OF ABBREVIATIONS & SYMBOLS USED

Gene and protein symbol conventions, as represented by "*cadherin 5/vascular endothelial cadherin*" gene

Species	Gene Symbol	Protein Symbol
Homo sapiens (human)	*CDH5* *(UPPERCASE ITALICS)*	CDH5 (UPPERCASE)
Mus musculus (mouse)	*Cdh5* *(Sentence case italics)*	Cdh5 (Sentence case)
Danio rerio (zebrafish)	*cdh5* *(lowercase italics)*	cdh5 (lowercase)

Units

dpf	days post fertilization
dpt	days post treatment
hpf	hours post fertilization
m_	milli_(10^{-3})
µ_	micro_(10^{-6})
n_	nano_(10^{-9})
v/v	volume by volume percentage solution
w/v	mass by volume percentage solution

Abbreviations & Symbols

ADME	absorption, administration, metabolism, excretion
AKT	protein kinase B
CDH5	*cadherin-5/VE-cadherin*
CNIB	Canadian National Institute for the Blind
CRISPR	clustered regularly interspaced short palindromic repeats
DMSO	dimethyl sulfoxide
dsred	*dicosoma red fluorescent protein*
EGFP	*enhanced green fluorescent protein*
FA	fluorescein angiography
FEVR	familial exudative vitreoretinopathy
flk1	*fetal liver kinase-1*
fli1a	*Fli-1 proto-oncogene, ETS transcription factor a*
FZD4	*frizzled class receptor-4*
gata1	*GATA-binding factor-1*
Gsk3β	glycogen synthase kinase 3 beta
HUVEC	human umbilical vein endothelial cells
IP	incontinentia pigmenti
IVFA	intravenous fluorescein angiography
KIF11	*kinesin family member-11*

LEF	lymphoid enhancing binding factor-1
LRP5	*low density lipo-protein receptor-related protein-5*
logSW	solubility of compound in water
MO	morpholino oligonucleotide
MLCRD	microcephaly, lymphedema, chorioretinal dysplasia
MTD	max tolerated dose
MTD-50	50% of MTD
NDP	Norrie disease protein
PCR	polymerase chain reaction
PFA	paraformaldehyde
PFV	persistent fetal vasculature
PI3K	phosphoinositide-3-kinase
PTU	1-phenyl-2-thiourea
RNA	ribonucleic acid
ROP	retinopathy of prematurity
S1PR1, 2, 3	sphingosine 1- phosphate receptor 1, 2, 3
SEM	standard error of the mean
TALEN	transcription activator-like effector nuclease
TCF	T-cell factor
Tg	*transgene*
TSPAN12	*tetraspanin-12*
UCLA	University Committee of Laboratory Animals
VEGF	vascular endothelial growth factor
Wnt	wingless (Wg)-related mouse mammary tumor virus (MMTV) integration site (**Int**)
WT	wildtype
ZNF408	*zinc finger protein-408*

ACKNOWLEDGEMENTS

First and foremost, I would like to thank my supervisors Dr. Johane Robitaille and Dr. Jason Berman. Together, you have made taking on a research project in a small time period less daunting. You both have taught me more than just the material in these pages. Thank you Dr. Robitaille for helping me pursue sources of funding and giving me the opportunity to be involved in your exciting world of research. Your passion for vision science did not go unnoticed and is something I admire. Thank you Dr. Berman for your dedication to my project. Your positive outlook and enthusiasm has guided me through many obstacles.

Thank you to my remaining committee members, Drs. Christopher McMaster and Shelby Steele. Thank you Dr. McMaster for sharing your expertise this past year. Thank you Dr. Steele for your patience with me, as this project did not come with ease. Your knowledge, passion, talent, and dedication has brought me through to the (almost) end. I could not have asked for a better research mentor. This committee was truly the ultimate multidisciplinary team.

To the Berman Zebrafish Laboratory members- I feel lucky to have been a part of such a great research family. Thank you to Dr. Mike Ngo, Dr. Gordon Simms, and Dr. Sergey Prykhozhij for guiding me in your areas of expertise.

Finally, I would like to sincerely thank Dr. William Baldridge for taking on the role of my external examiner. I appreciate your time and effort and hope this thesis proves to be an enjoyable read.

I would like to acknowledge the Dr. R. Evatt and Rita Mathers Trainee Award as a source of funding.

CHAPTER 1: INTRODUCTION

1.1 Human retinal development

The retina is a light sensitive tissue located at the back of the eye and is considered a part of the central nervous system, specifically, an out-pouching of the diencephalon. In a normal eye, light is focused on the retina by the cornea and lens, to construct a clear image for the brain to interpret. When light hits the retina, signaling cascades are induced with the help of cells and neurons interconnected by synapses, including rod and cone photoreceptors (Kennis & Mathes, 2013). These photoreceptors are sensitive to light rays. Visual signals are eventually sent to the brain via optic nerve fibers and processed in various areas of the brain to allow for visual interpretation of the environment that one sees (Behnia & Desplan, 2015). The retina is supplied with nutrients and oxygen early on in embryogenesis from several vascular networks that are highly complex and coordinated developmental events (Hughes et al., 2000). If any step during development is compromised, this can consequently have a negative impact on visual acuity and may result in variety of retinal pathologies.

The human ocular vascular system arises from mesoderm that surrounds the newly formed optic cup during embryogenesis (Saint-Geneiz & D'Amore, 2004). Prior to the initiation of retinal vascularization, at 4 weeks gestation, the primitive dorsal and ventral ophthalmic arteries branch from the internal carotid artery (Saint-Geneiz & D'Amore, 2004). Hyaloid, retinal, and choroidal vasculature blood vessel networks arise from these vessels and are the three main networks that are necessary to supply the retina and are formed via angiogenesis, a process by which new blood vessels form from pre-existing vessels (Saint-Geniez & D'Amore, 2004). The hyaloid and choroidal vascular

systems begin development before the retinal vascular network and thus are initially responsible for nourishing retinal tissue in its earliest stages of embryogenesis.

The hyaloid network is the first to form and nourishes the developing retina prior to blood vessels entering the retina. The primitive hyaloid artery travels through the optic fissure during development and reaches the lens at the 7 mm stage (human developmental stage) where it branches into a close-knit vascular network around the lens (Saint Geniez & D'Amore, 2004). The hyaloid vasculature exists only transiently and begins to regress at approximately 13 gestational weeks, corresponding to the onset of retinal vascular development (Saint Geniez & D'Amore, 2004), and is usually completely regressed by 40 weeks, when retinal vascularization is complete (Gilmour, 2015).

Vascularization of the neural retina itself begins at approximately 18 weeks gestation and is normally complete between 38 and 48 weeks gestation (Gilmour, 2015). Mesenchymal precursor cells from the vascular plexus (network) migrate to the nerve fiber layer and subsequently proliferate to form cords of endothelial cells, referred to as vasculogenesis (Garner & Klintworth, 2008). The retinal vascular network is made up of a superficial primary and a deep secondary vessel system (**Figure 1.1**) (Hughes, 2000) that feed the inner and middle layers of the neural retina. Primary vasculature matures into arteries and veins, undergoes pruning, and pericytes eventually wrap around endothelial cells, stabilizing new vessels (Bergers & Song, 2005; Hughes et al., 2000). Following vasculogenesis, angiogenesis occurs creating the secondary vascular network whereby new vessels form from pre-existing ones, increasing the network density (Hughes et al., 2000). Patterning of the vascular endothelium is influenced by vascular endothelial growth factor (VEGF) providing guidance cues and is present in a spatio-

temporal distinct manner and is also influenced by levels of oxygen (Garner & Klintworth, 2008). Retinal development is conveniently depicted using retinal whole mounts showing that the retinal vasculature emerges from the optic disk area, where the vessels project radially outward toward the periphery (**Figure 1.1**). The retina undergoes further maturation after birth (Hughes et al., 2000; Garner & Klintworth, 2008).

Retinal vascularization is a tightly regulated process that if disturbed at any step, may result in abnormal vascularization of the retina and subsequent vision loss or blindness. Persistent fetal vasculature (PFV) occurs when the hyaloid artery fails to regress and a membrane or stalk connecting the optic nerve and lens remains, leading to a variety of visual consequences. Retinopathy of prematurity (ROP) occurs when babies are born before the retina has time to fully develop, with the two major risk factors being the gestational age at birth and need for supplemental oxygen that suppresses growth factors and subsequently inhibits normal vessel growth, resulting in pathological retinal vascularization (Chen & Smith, 2007). Failure of peripheral vascularization can occur as a result of genetic insult such as in familial exudative vitreoretinopathy (FEVR). Interestingly, microphthalmia (abnormally small eyes) is frequently associated with retinal vascular disorders such as ROP, PFV, and FEVR (Hu et al., 2016; Goldberg, 1997; Robitaille et al., 2009). In ROP, peripheral vascularization can be completely absent and is positively correlated to both the incidence and severity of refractive error (the inability of the eye to properly refract and focus light rays, resulting in blurry vision), as well as delays in eye growth (Fledelius & Fledelius, 2012; Ouyang et al., 2015; Wang et al., 2013). PFV, ROP, FEVR and other retina vascular disorders such as Coat's disease (characterized by retinal telangiectasis/dilation) and incontinentia pigmenti (IP- a

multi-system disorder possessing some ocular characteristics such as neovascularization) have overlapping phenotypes, and all can lead to blinding complications that may require enucleation of the eye in the most severe cases (Hu et al., 2016; Gilmour, 2015). ROP is a leading cause of blindness in developed countries and an emerging problem in developing nations (Holmstrom et al., 1998). It is estimated that blindness affects at least ~20 000 prematurely born infants worldwide each year, of which at least 50% can be attributed to the severity of ROP (Blencowe et al., 2010). FEVR is associated with a 40% chance of vision loss in eyes of affected patients, with 50% of those patients becoming bilaterally legally blind, most often in early childhood years and despite treatment (Robitaille et al., 2011). In 2007, the National Coalition for Vision Health reported that the total annual cost of vision loss in Canada was approximately $15.8 billion and is projected to reach up to $30.3 billion in the year 2032 (www.cos-sco.ca). The Canadian National Institute for the Blind (CNIB) also reported that approximately half a million Canadians currently live with vision loss significant enough to negatively impact their quality of life. This highlights the importance of visual research and the need to expand knowledge of the pathological mechanism, treatment, and management of such diseases contributing to these statistics, and to manage them as efficiently as possible while still providing optimal ocular care (www.cnib.ca).

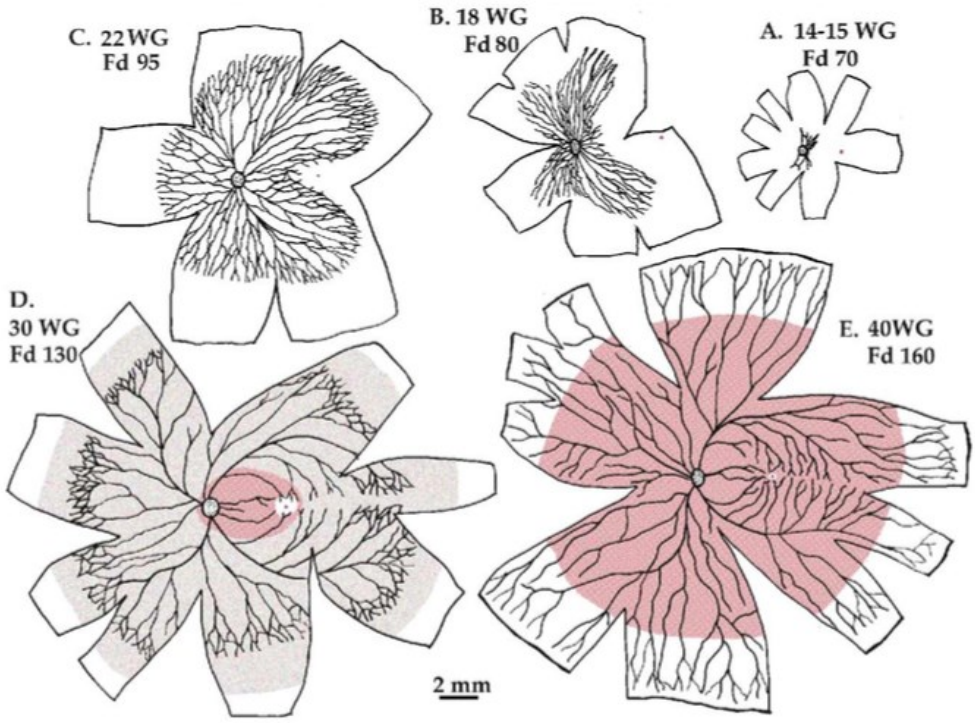

Figure 1.1. Human retinal vasculature emerges from the optic disc to periphery during development.

Human retinal vascular development is compared to that of macaque monkey retinal development through a retinal whole mount schematic. WG (human)- weeks gestation. Fd (monkey)- fetal day. Black lines represent vessels from primary vasculature and pink shading represents deep secondary or deep vasculature. The fovea (responsible for sharp, central vision) is indicated by a dot. The primary vessels begin to develop near the optic disk and the secondary vessels sprout from this primary layer. Vessels emanate from the optic disk to the peripheral retina (A-E). The primary vessel development in macaque monkeys is faster than humans (grey shading in D). Adapted from (Provis, 2001).

1.2 Familial exudative vitreoretinopathy (FEVR)

FEVR is a hereditary, developmental retina vascular disorder that is characterized by incomplete peripheral retinal vascularization at birth in both eyes and was originally described by Criswick and Schepens in 1969 (Criswick & Schepens, 1969) as resembling ROP but lacking a history of premature birth. In the first and earliest stage of FEVR, the retinal vessels fail to reach the ora serrata, a landmark of the eye described as the junction between the retina and ciliary body (Alvarez et al., 2007). Individuals with FEVR manifesting as peripheral avascular retina may not experience visual symptoms and may not be aware that they have the condition, yet are at risk of having children who may become blind from the disease. Visual complications occur when the second stage of disease begins. The second stage is induced by retinal ischemia (reduced blood flow), caused by the peripheral avascular area leading to secondary neovascularization (ie. new, abnormal vessel growth). This compensatory neovascularization phase is not specific to FEVR and occurs because of the presence of avascular retina. Neo-vessels are not normal vessels and are characterized by increased permeability with associated leakage and hemorrhage and eventually scar and cause traction on the retina (Alvarez et al., 2007). Traction often involves the macula and may manifest as retinal dragging and with further traction, eventually lead to retinal folds and detachment.

FEVR is phenotypically variable. Although both eyes are typically affected, asymmetry between eyes and variability of disease severity between immediate family members may be present depending on the extent of the disease caused by the second stage of neovascularization (Gilmour, 2015). FEVR is believed to have 100% penetrance and can be progressive later in life, adding to the variability and unpredictable nature of

the disease (Toomes et al., 2004; Shukla et al., 2003; Gologorsky, Chang, Hess, Berrocal, 2013). The prevalence of FEVR has been estimated at 1:10 000, but this is likely an underestimate as studies utilizing molecular testing reveal that, in some pedigrees, up to 90% of individuals with FEVR may be asymptomatic (Toomes & Downey, 2011). The resulting visual acuity deficits range from visual impairment to total blindness despite current treatments (e.g. laser and vitreoretinal surgery). Approximately 21-64% of FEVR affected patients will experience a retinal detachment (van Nouhuys, 1991; Miyakubo, et al., 1984; Benson, 1995; Ranchod, et al., 2011; Shukla, et al., 2003). In one study which looked at 32 patients (64 eyes) diagnosed with FEVR, 3% were observed to have no light perception, 16% were considered legally blind (defined as 6/15 visual acuity or worse), and 6% had some visual impairment with a visual acuity worse than 6/15 but better than 20/200 (Robitaille et al., 2011).

Imaging of the retina through the pupil, referred to as a fundus photo, can show a wide view of the retina and its corresponding vasculature. **Figure 1.2** compares the retinal phenotype of an unaffected person to that of a patient diagnosed with FEVR. In the unaffected person, one can see that the retinal vessels are organized and clearly defined as they emerge from the optic disc (**Figure 1.2A**, arrow). By contrast, the patient affected with FEVR has a severe form of the disease and displays a lack of organization with no visible retinal vessels, as well as a large fibro-vascular stalk emanating from the optic nerve (**Figure 1.2B**, arrow). This patient with FEVR has an easily detectable pathological appearance, but this is not the case for all patients with FEVR: some will have a normal fundus as in **Figure 1.2A** and will require a fluorescein angiogram (FA)

that involves injecting a dye that highlights the retina vessels and enables the detection of the area of peripheral avascular retina.

In those patients with low vision, there is also a risk of developing strabismus, otherwise known as abnormal alignment of the eyes (**Figure 1.3**), and microphthalmia, which further complicates patient management and introduces the potential need for multiple surgical interventions.

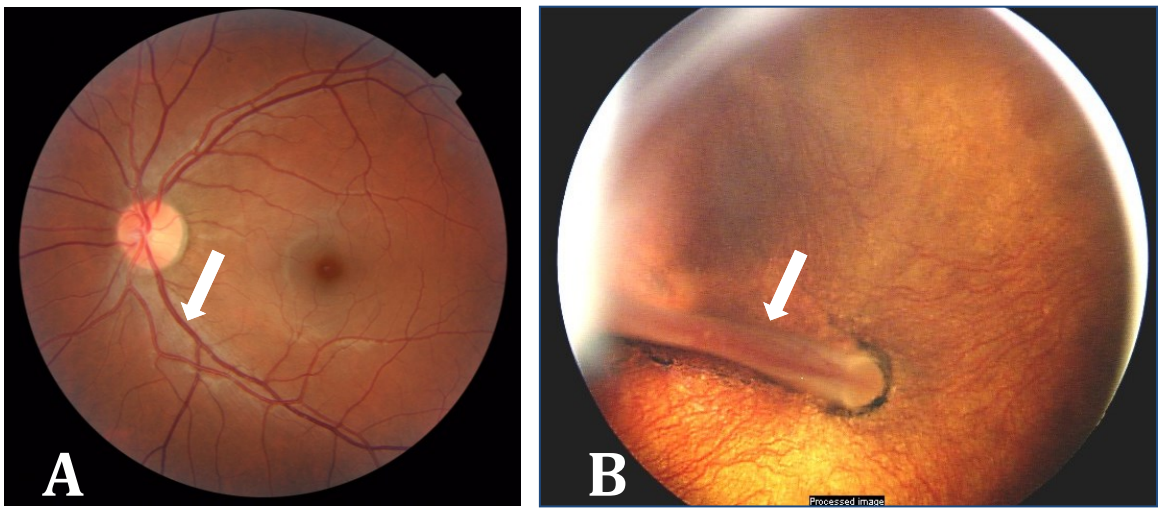

Figure 1.2. Comparison between normal retina and severe FEVR phenotype.

A- Normal human fundus with retinal vessels emerging from the optic nerve and coursing outward toward the periphery. Arrow indicates one of the many healthy vessels on this retina. B- Fundus of a patient with FEVR with a noticeable fibro-vascular stalk extending from the optic nerve (indicated by the arrow). There are no visible retinal vessels. Adapted from (Robitaille et al., 2009).

Figure 1.3. Strabismus in a severely affected FEVR patient.

A view of the outside of the eyes shows the presence of leukocoria, or white pupil, due to a total retinal detachment in both eyes as a consequence of FEVR. The eyes also appear to have strabismus, or an eye misalignment, when comparing the light reflexes in each eye. This patient has an exotropia (ie. the eyes are deviated outward). Adapted from (Toomes et al., 2004).

A staging system has been proposed (**Table 1.1**) to describe the degree of severity of FEVR. This system ranges from stage one manifesting (avascular periphery only) and being the least severe to stage five, the most severe (with total loss of vision secondary to a total retinal detachment) (Pendergast et al., 1998; Gilmour, 2015). Older children and adults, whom the peripheral retina only is affected and no symptoms are present, are observed and need for treatment is unlikely (Laqua, 1980). The more severe stages tend to occur early in childhood years. Retinal dragging and detachment are difficult to treat and may require a vitrectomy, to remove the vitreous humor (the jelly-like substance occupying the space behind the lens in the eye) from the eye (Cruz-Inigo et al., 2014). All fibrovascular tissue would be removed from the eye to relieve traction and the vitreous would be replaced with a suitable substance (Cruz-Inigo et al., 2014). Severe cases may also need scleral buckling, a technique used to close a retinal break and release traction (Laqua, 1980).

Table 1.1. Clinical staging of FEVR.

Stage	Description
1	Avascular periphery
2	Retinal neovascularization
	A- without exudates
	B- with exudates
3	Extra macular retinal detachment
	A- without exudates
	B- with exudates
4	Subtotal macula involving retinal detachment
	A- without exudates
	B- with exudates
5	Total retinal detachment

Adapted from (Pendergast & Trese, 1998; Gilmour, 2015)

Due to the significant phenotypic overlap between FEVR and ROP, a history of premature birth must be elicited before a diagnosis of FEVR can be entertained. Other conditions in the differential diagnosis of FEVR include Norrie disease, an X-linked recessive condition associated with progressive deafness and mental retardation (Warburg, 1966), PFV, which presents unilaterally in an eye and is rarely inherited (Haddad et al., 1978), incontinentia pigmenti (IP), an X-linked dominant disorder of the skin with similar ocular manifestations to FEVR, osteoporosis pseudo-glioma (OPPG), which has the additional presence of osteoporosis that differentiates it from FEVR (Gilmour, 2015), microcephaly, lymphedema, chorioretinal dysplasia (MLCRD), Coat's disease, which is frequently unilateral, rarely hereditary and with a male predilection (Warden et al., 2007). The ocular manifestations of FEVR are non specific and a thorough work-up that may include molecular testing is essential to make the correct diagnosis.

1.3 Genetic etiology of FEVR

Recent studies have focused on the genetic etiology of FEVR. To date, six genes have been identified, and patients with suspected FEVR may now undergo genetic testing to confirm the diagnosis and rule out other forms of retinal vascular disease. Mutations in Frizzled-4 protein (*FZD4*) (Robitaille et al., 2002), low density lipo-protein receptor related protein-5 (*LRP5*) (Gilmour, 2015), tetraspanin-12 (*TSPAN12)* (Gal et al., 2014), Norrie disease protein (*NDP*) (Rattner et al., 2014), kinesin family member-11 (*KIF11*) (Robitaille et al., 2014), and zinc finger protein-408 (*ZNF408*) (Collin et al., 2013; Gilmour, 2015) have all been linked to FEVR. FEVR is genetically heterogeneous and is

most commonly inherited as an autosomal dominant (AD) trait (*FZD4*, *LRP5*, *TSPAN12*, *ZNF408*, *KIF11*), but may also follow X-linked recessive (*NDP*), or, autosomal recessive inheritance (*FZD4*, *LRP5* and *TSPAN12*) (Muller et al., 1994; Robitaille et al., 2002; Norrie, 1927; Jaio et al., 2004; Poulter et al., 2010; Collin et al., 2013, Gilmour, 2015). Most reported cases of AD FEVR are associated with heterozygous mutations in *FZD4* (20%) or *LRP5* (15%) (Toomes et al., 2004).

Extraocular manifestations are rare with the exception of FEVR caused by *LRP5* and *KIF11* mutations. Pedigrees with heterozygous mutations in *LRP5* were discovered to have reduced bone density and an increased incidence of bone fractures (Toomes et al., 2004). Interestingly, homozygous mutations in *LRP5* have been identified in patients with osteoporosis-pseudoglioma syndrome, a condition characterized by severe loss of bone density and a gliomatous appearance in the eyes that represents an end-stage FEVR phenotype (Laine et al., 2011). Those possessing *KIF11* mutations appear to have FEVR ocular manifestations as well as frequent associations with microcephaly, lymphedema, and mental retardation (Hu et al., 2016). Also, mutations in the *NDP* gene have been associated with Norrie disease, FEVR, or both (ie. some relatives with the same mutation exhibiting Norrie disease and others FEVR only) (Allen et al., 2006), highlighting the phenotypic variability of the disease.

The *FZD4* gene was originally identified as causative of FEVR in a multigenerational pedigree in 2002 (Robitaille et al., 2002). *Fzd4* $^{-/-}$ knockout mice, the most thoroughly studied of the FEVR mouse models, recapitulate the human phenotype and display delayed regression of the hyaloid vascular system as well as an overall retinal vascular disorganization and failure of complete vascularization (Xu et al., 2004;

Ye et al., 2009). Interestingly, *Fzd4* $^{-/-}$ mice also show evidence of progressive cerebellar degeneration, a feature not found in humans with FEVR cause by *FZD4* mutation (Wang et al., 2001). Behavioural studies in FEVR mouse models have demonstrated that *Fzd4* mutations are associated with abnormal optokinetic reflex (innate reflex eye movements that may be used as a measure of the ability to see) (Ye et al., 2009). *Lrp5*, *Tspan12* and *Ndp* null mice also demonstrate abnormal retina vascular development as seen in human FEVR patients (Xia et al., 2008; Junge et al., 2009; Richter et al., 1998).

Four of the confirmed genes form a ligand/frizzled receptor/co-receptor complex: (*NDP/FZD4/LRP5/TSPAN12*). Proteins encoded by these genes participate in the canonical-Wnt intracellular signaling pathway (**Figure 1.4**). In general, the Wnt signaling pathway is involved in cell fate, i.e. how cells and tissues are instructed to develop, as well as the repair of adult tissues (Clevers, 2009). In the eye, this pathway has emerged as a key player in the regulation of retinal vascular development (Xia et al., 2010). FZD4 is a 7 transmembrane domain receptor and belongs to the canonical norrin-Wnt signaling pathway (Warden et al., 2007). *NDP* produces norrin that acts as a non-Wnt ligand with high specificity for Frizzled-4 at the cellular plasma membrane, and tetraspanin-12 aids Frizzled-4 to potentiate intracellular signaling (Xu et al., 2004). FZD4 and LRP5 act as co-receptors and are both necessary to initiate intracellular signaling (Xu et al., 2004). Downstream events that occur in this pathway are not clearly defined and therefore may represent as yet unknown causes of FEVR pathology (Xu et al., 2004). Indeed, about 50% of FEVR cases do not have a genetic etiology, suggesting that more genes for FEVR remain unidentified (Seo et al., 2015).

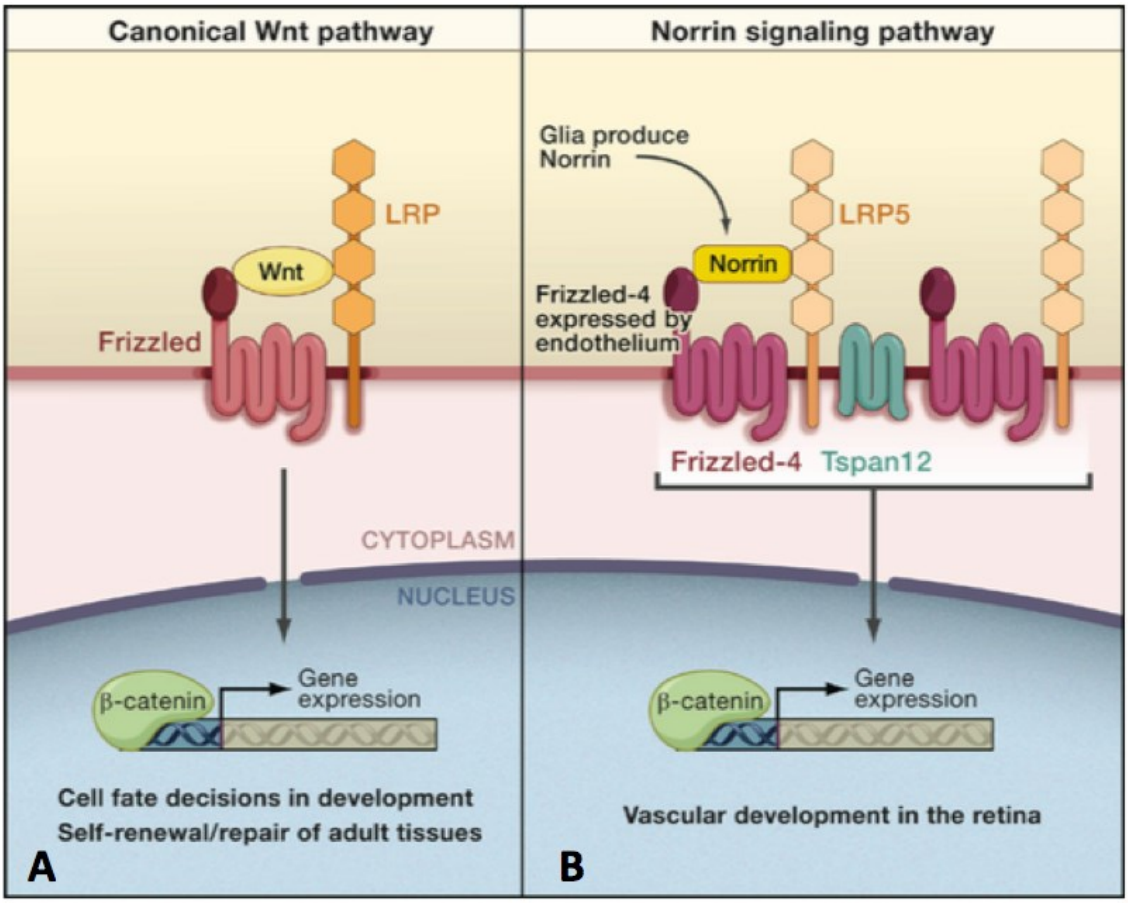

Figure 1.4. FEVR genes play a role in the canonical Wnt pathway.

A- Globally, Wnt ligands bind to their associated Frizzled receptors and the co-receptors Lrp5 or Lrp6 in organisms. Upon activation by the ligand, β-catenin becomes activated downstream and further activates gene expression to regulate a variety of processes in both embryo and adults. B- In the retina, vascular development is regulated by the binding of the ligand Norrin to the Frizzled-4 Wnt receptor and its Lrp5 co-receptor located on endothelial cells. A complex is then formed with Tspan12, which activates downstream β-catenin signaling.
Adapted from (Clevers, 2009).

1.4 *CDH5*- a novel FEVR gene

CDH5, which codes for the VE-cadherin (vascular endothelial-cadherin) protein, is one such newly identified potential FEVR gene (Dr. Johane Robitaille, personal communication, manuscript in preparation). It was first identified in a French Canadian family that had no mutation in the known FEVR genes using whole exome sequencing. Cadherins are transmembrane proteins composed of an extracellular domain, which participates in cell-to-cell interactions, and a cytoplasmic tail, which interacts with catenins (Wheelock & Johnson, 2003). VE- cadherin is the major cadherin present in the adherens junctions of endothelial cells, which line the vasculature (Wheelock & Johnson, 2003). It has an important role in maintaining adhesion of endothelial cells, restraining endothelial cell proliferation, and controlling vascular permeability (Breviario et al., 1995; Caveda et al., 1996). *CDH5* also plays a role in regulating the availability of β-catenin, the transcription factor activated by Wnt signaling, possibly by sequestering it, which may provide a link between this protein and the FZD4 signaling pathway and thus, the retinal pathology of FEVR (Wheelock & Johnson, 2003). VE-cadherin binding to β-catenin, allows for the association of cadherin with actin, providing support to the cytoskeleton (Wheelock & Johnson, 2003). Homozygous inactivation of *Cdh5* in mice has resulted in embryonic lethality due to severe cardiovascular defects, whereas heterozygous $Cdh5^{+/-}$ mice were described as normal (Carmeliet et al., 1999; Gory-Faure et al., 1999). Blood vessel integrity is defective in VE-cadherin knockout mice, which were isolated at various stages of gestation (Gory-Faure et al., 1999), and knockout mice show severely abnormal angiogenesis during development, implying that VE-cadherin may be involved in more than just cell-to-cell adhesion (Carmeliet et al., 1999). A

vascular maintenance role has been shown in mouse embryos deficient in VE-cadherin in-utero (Gory-Faure et al., 1999). Interestingly, suppression of Cdh5 by treating mice with tamoxifen to induce recombination resulted in hyper-sprouting of retinal vasculature (Gaengel et al., 2012). In *cdh5* zebrafish mutants, studies identified that there was overall disorganization of the actin cytoskeleton (Sauteur et al., 2014), and that c*dh5* is important for structural support for polymerizing F-actin cables involved in endothelial cell elongation in zebrafish (Sauteur et al., 2014). Sauteur and colleagues (2014) concluded that *cdh5* is necessary for global blood vessel integrity and vessel sprouting.

To date, no treatment is available to address the underlying pathology in FEVR prior to development of compensatory neovascularization and subsequent blinding complications. Management depends on the stage/severity of FEVR and can range from continued lifelong observation to laser photocoagulation and vitreoretinal surgery. Surgical complications are frequently encountered, and success rates tend to be low in younger patients, highlighting the need to identify effective treatments that will foster normal vascularization of the peripheral retina in patients with FEVR, thus avoiding the difficulties of treating complications of secondary neovascularization with poor success rates. It is possible that the FEVR phenotype could be reversed by targeting pathways that influence blood vessel development.

Angiogenesis is controlled by multiple signaling pathways. We were interested in exploring how altering other signaling pathways involved in angiogenesis might be used to reverse the underlying vascular pathology in FEVR.

1.5 Sphingosine-1-phosphate (S1P) receptors and JTE-013

The S1P signaling pathway is known to play a role in angiogenesis via the S1P family of G-protein coupled receptors (S1PRs) and serves as an attractive target to treat vascular disease (S1PRs) (Skoura et al., 2007). S1P is a blood borne lipid mediator that regulates multiple physiological processes including vascular morphogenesis and maturation (Hisano et al., 2015). S1P (produced primarily by endothelial cells) interacts with S1PRs which then activate downstream signaling pathways (Hisano et al., 2015). S1PRs have 7 transmembrane domains with three extracellular loops (Hanson, 2012). Mammals possess 5 S1PRs but only S1PR1, 2 and 3 have been linked to vascular development and each binds to a different hetero-trimeric G-protein α-subunit (Kono et al., 2004; Hanson, 2012). S1PR1 and 3 have been reported to have a similar role in blood vessel development, promoting vascular stability and increasing vascular migration upon S1P ligand binding (Kono et al., 2004). In contrast, S1PR2 is an inhibitor of vascular development and therefore possesses an antagonizing effect against S1PR1 and 3 (**Figure 1.5**). S1PR2 would be a suitable candidate to test whether blocking this receptor might foster vessel growth in patients with FEVR.

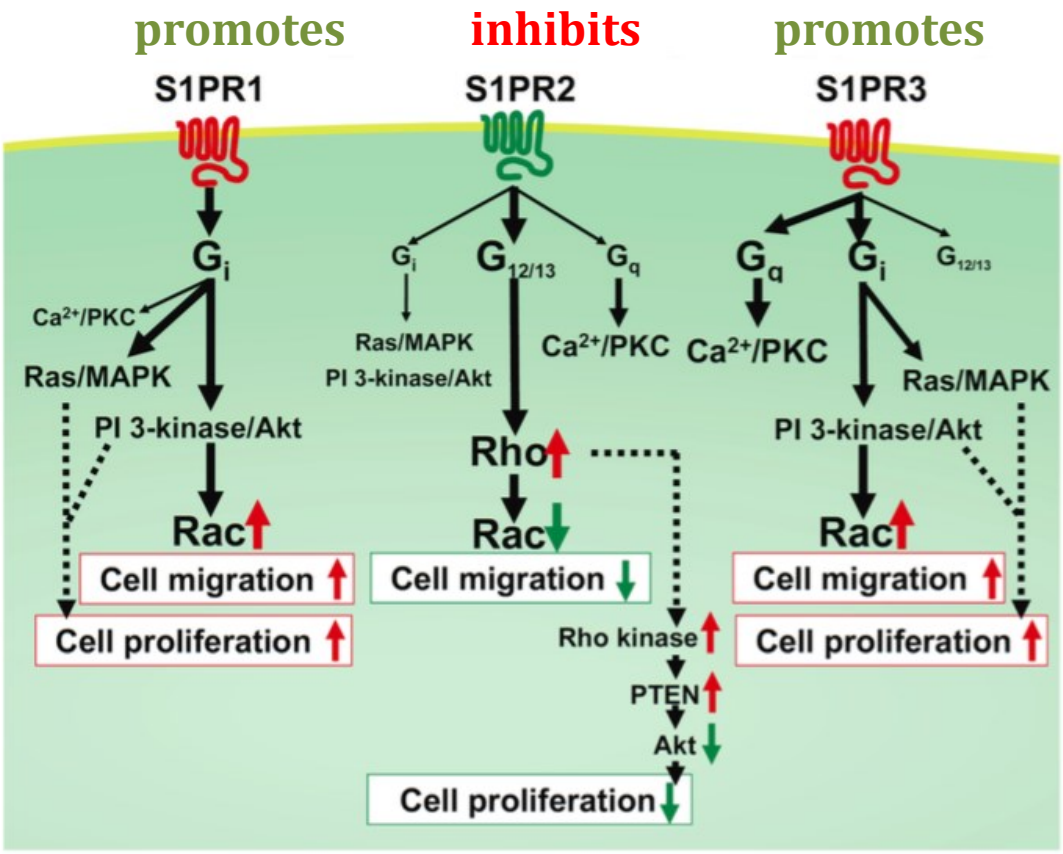

Figure 1.5. S1PR2 inhibits vascular development while S1PR1 and S1PR3 promote vessel growth.

Blocking receptor 2 could promote vascularization by preventing inhibition of vessel growth. Adapted from (Takuwa et al., 2011).

S1pr2$^{-/-}$ null mice develop normally (Skoura et al., 2007), suggesting that targeting this receptor as a treatment for FEVR might not have significant unwanted side effects. When exposed to ischemia-driven retinopathy (used to mimic ROP and diabetic retinopathy). The *S1pr2*$^{-/-}$ mice appear to be protected against the development of retinal vascular abnormalities (Skoura et al., 2007). Offspring of *S1pr2*$^{-/-}$ mice crossed with either *Fzd4*$^{-/-}$ *or Tspan 12*$^{-/-}$ mice show near normal retinal vascularization compared to *Fzd4*$^{-/-}$ and *Tspan 12*$^{-/-}$ mice (Mike Ngo, Dalhousie University, unpublished data). Taken together, this suggests that S1PR2 represents a valid, druggable target to inhibit pathological neovascularization in conditions such as FEVR.

The compound JTE-013 is a well-established S1P antagonist with a higher specificity for S1PR2 when compared to S1PR1 or 3 (Won et al., 2012). Unfortunately, JTE-013 possesses several non-drug like properties (ie. rapid metabolism) thus, preventing its use in vivo. The recent availability of the crystal structure of S1PR2 has enabled homology modeling to allow for accurate determination of the structure of the receptor family (Christopher McMaster, personal communication). This has facilitated the prediction of drug-like compounds that have a high affinity for the S1PR2 receptor. The Cheminformatics Drug Discovery Lab (CDDL) at the IWK Health Centre run by Dr. Christopher McMaster and his team screened a proprietary database of 11.5 million drug-like compounds to identify 15 compounds predicted to have high affinity for S1PR2 (**Table 1.2**).

Screening large numbers of compounds for their ability to target specific proteins and thus produce readable phenotypic outcomes is made easier by the use of animal models of specific diseases. Mice have commonly been used for this purpose, however

this model has several limitations, including the high expense of maintenance, as well as low fecundity, which can limit the numbers of animals necessary for large-scale drug screens. The introduction of the zebrafish into the realm of pre-clinical animal models of disease has streamlined and revolutionized the process of drug discovery ultimately improving efficiency.

Table 1.2. Molecular modeling of S1PR2 binding pocket predicted this list of S1PR2 antagonists.

Compound Name	Molecular Weight (g/mol)
4-cyclopropyl-N-(3,4-dimethoxybenzyl)-1,3-dimethyl-1H-pyrazolo[3,4-b]pyridine-6-carboxamide	380.4
N-[1-(1H-benzimidazol-2-yl)ethyl]-1,3,6-trimethyl-1H-pyrazolo[3,4-d]pyrimidin-4-amine	321.4
2,6-dichloro-N-{[(3,4-dichlorophenyl)amino]carbonyl}-4-methyl-5-nitronicotinamide	438
2,6-dichloro-4-methyl-N-({[2-(trifluoromethyl)phenyl]amino}carbonyl)nicotinamide	392.2
4-cyclopropyl-1,3-dimethyl-N-[4-(trifluoromethyl)phenyl]-1H-pyrazolo[3,4-b]pyridine-6-carboxamide	374.4
2,6-dichloro-N-[2-(3,4-diethoxyphenyl)ethyl]-4-methylnicotinamide	397.3
2,6-dichloro-N-[(mesitylamino)carbonyl]-4-methylnicotinamide	366.2
N-[(benzylamino)carbonyl]-2,6-dichloro-4-methylnicotinamide	338.2
N-(4-chlorophenyl)-4-cyclopropyl-1,3-dimethyl-1H-pyrazolo[3,4-b]pyridine-6-carboxamide	340.8
2,5,6-trichloro-4-methyl-N-{[(2-phenylethyl)amino]carbonyl}nicotinamide	386.7
methyl (2S)-[(6-isopropyl-1-methyl-1H-pyrazolo[3,4-d]pyrimidin-4-yl)amino](phenyl)acetate	339.4
2,6-dichloro-N-{[(2-ethylphenyl)amino]carbonyl}-4-methylnicotinamide	352.2
2,6-dichloro-N-{[(2,5-dichlorophenyl)amino]carbonyl}-4-methylnicotinamide	393.1
N-benzyl-2,6-dichloro-N-ethyl-4-methylpyridine-3-sulfonamide	359.3
4-cyclopropyl-N-(4-isoxazol-5-ylphenyl)-1,3-dimethyl-1H-pyrazolo[3,4-b]pyridine-6-carboxamide	373.4

1.6 Zebrafish as a preclinical FEVR model

Zebrafish (*Danio rerio*) are an excellent pre-clinical vertebrate model due to their high fecundity rate, small size, external fertilization, optically transparent embryos, cost effectiveness compared to rodents, rapid embryogenesis and development. In addition, they have a fully sequenced genome and this is constantly updated with new versions as part of the Zebrafish Genome Project (Zon & Peterson, 2005). Zebrafish reach sexual maturity by approximately three months, breed frequently, and produce 200-300 embryos per female per breeding (Jing & Zon, 2011; Zon, 1999). Organ development in zebrafish also closely resembles that of humans, with multiple organ systems being driven by the same genetic and physiological mechanisms (Williams & Hong, 2011).

1.7 Zebrafish retinal development

Zebrafish retinal development is more rapid and simple than in humans, with a functional retina presenting by 3 days post fertilization (dpf) (Easter & Nicola, 1996). In contrast to human retinal development, the zebrafish embryonic vasculature is hypothesized to transition into a mature retinal network where vessels gradually move away from the lens and onto the retina as opposed to degenerating then re-generating into a mature vessel network (Kitambi et al., 2009). Zebrafish do not have an avascular region corresponding to cone-enriched fovea as would be seen in mammalian eyes (Alvarez et al., 2007). Another distinguishing feature of the zebrafish retina is the absence of intra-retinal capillaries that form within the inner and outer plexiform layers (Alvarez et al., 2007). It is thought that this does not occur because the zebrafish retina is

considerably thinner than a human retina. Despite these differences, there are also several similarities between humans and zebrafish that advocate the use of them as a tool in this study (**Table 1.3**). The zebrafish eye can easily be viewed using histology (**Figure 1.6 A**). Both organisms have primitive retinal vasculature that branches via angiogenesis from a central retinal artery, both possess a hyaloid vascular layer tightly associated with the lens early in development (**Figure 1.6 B**), and both have vasculature enriched in pericytes (Alvarez et al., 2007).

At approximately 18 hours post fertilization (hpf) the zebrafish embryo begins to form the choroid fissure and simultaneously, the eyecup begins to invaginate (Kitambi et al., 2009). By 24 hpf, the presence of retinal cells in the choroid fissure can be detected and later, at 27 hpf, post mitotic ganglion cell progenitors indicate the beginning of neurogenesis of the retinal layers (Kitambi et al., 2009). At 28 hpf, zebrafish endothelial cells start to move from the choroid fissure to an area behind the developing lens (Kitambi et al., 2009). Finally at 48 hpf, blood vessels can be found surrounding the medial side of the developing lens followed by expansion and fusion into a ring vessel, which will eventually surround the lens during the next 24 hours (Kitambi et al., 2009). The blood vessel network in the mature zebrafish eye is comprised of three radial vessels referred to as nasal, dorsal, and ventral, which branch off from the ring vessel. Throughout the final stages of ocular embryogenesis in both humans and zebrafish, the vessels continue to undergo remodeling and become increasingly less convoluted (Kitambi et al., 2009). Once the final plexus of blood vessels has surrounded the outer eye surface, blood circulation in the larval retina is visible at around 72 hpf/3 dpf (Kitambi et al., 2009).

Table 1.3. Zebrafish and human retina share several similarities and differences. ✓= indicates possession, ✗= indicates absence.

Retinal Characteristic	Human	Zebrafish
vasculature rich in pericytes (contractile cells that wrap around the endothelial cells of capillaries)	✓	✓
hyaloid vasculature tightly associated with lens early in development	✓	✓
primitive retinal vasculature branches via angiogenesis from central retinal artery	✓	✓
thin retina	✗	✓
hyaloid vascular system transforms into mature retina vasculature, instead of completely regressing	✗	✓
intra-retinal capillaries that form inner & outer plexiform layers	✓	✗

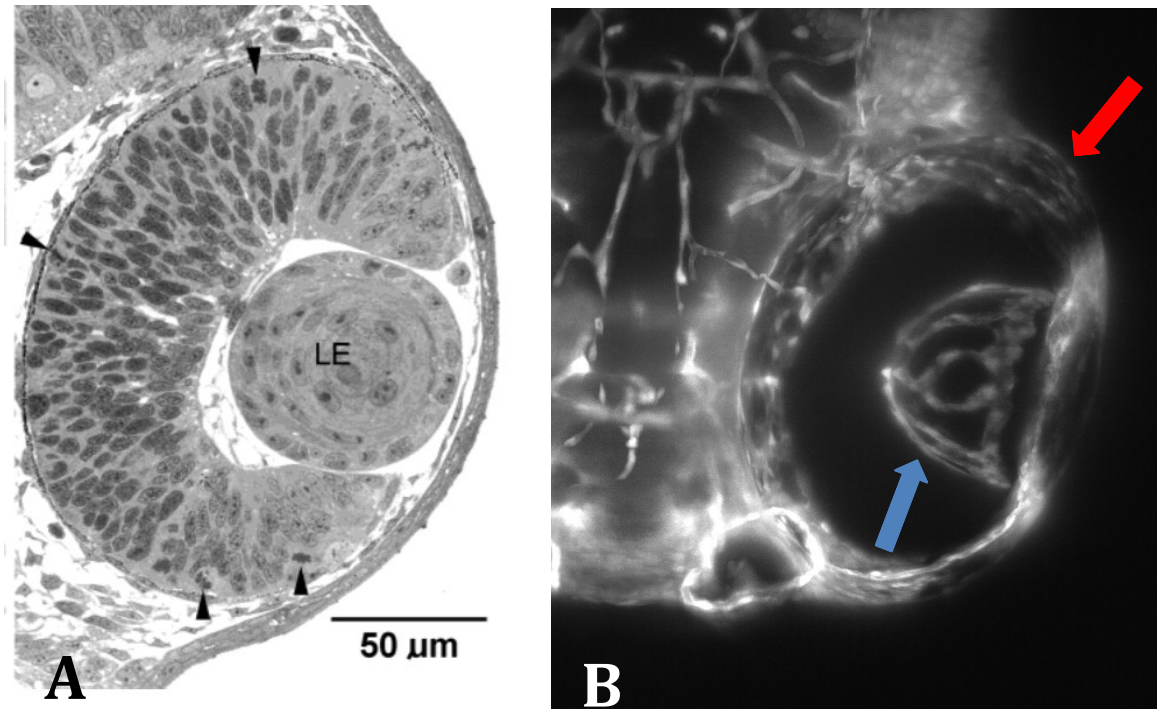

Figure 1.6. WT zebrafish eye histology and vascular anatomy.

A- Photomicrograph of a zebrafish eye at 36 hpf (LE-lens). Adapted from (Li et al., 2000). Neural tissue is seen surrounding the lens. Similarities can be seen between anatomical landmarks between A and B. B- Top red arrow indicates the outside border of the 3 dpf zebrafish eye and is referred to as "area outer eye" in future descriptions. The bottom blue arrow indicates the retinal vascular network tightly associated with the lens, referred to as "area inner eye" in future descriptions, which will eventually transition into a mature retinal network at the back of the eye. Image captured using Zeiss Lightsheet Z.1 connected to two PCO edge 5.5 sCMO cameras.

1.8 Zebrafish gene manipulation to create mutants and morphants

Another great utility of the zebrafish model is the availability of transgenic lines, which facilitate the visualization of developing structures by driving fluorescent protein expression under tissue-specific promoters. For example, to aid in the visualization of vasculature in the zebrafish, including that of the retina, *Tg*(*fli1a*:*EGFP*) zebrafish can be used that express green fluorescent protein (GFP) driven by the presence of *fli-1 proto-oncogene, ETS transcription factor-a (fli1a)* in the vascular endothelium (Lawson & Weinstein, 2002). The *fetal liver kinase-1* (*flk1)* promoter can also be used in place of the *fli1a* promoter to highlight the vascular endothelium (Gore et al., 2012). Numerous vascular studies have used this transgenic line followed by gene manipulation to study vascular disease such as ROP, Coat's disease, and general vascular development, as these embryos can be placed under a microscope and all vasculature will be highlighted by GFP (Wu et al., 2015; Collin et al., 2013; Hartsock et al., 2014).

Approximately 70% of all human disease genes have a functional homolog in zebrafish and can be relatively easily genetically manipulated when compared to murine models (Langheinrich U., 2003; Howe et al., 2013). For instance, the FEVR gene *TSPAN12* in humans shares 70% of its identity with zebrafish, and Norrin orthologs share approximately 68.6% conservation (Junge et al., 2009). The human genes *CDH5* (39% homology) (Larson et al., 2004), *FZD4* (84% homology) (BLASTP analysis, ensembl.org), and *S1PR2* (60% homology) (BLASTP analysis, ensembl.org) all have a zebrafish counterpart.

Gene-specific targeting using morpholino (MO) oligonucleotides is a standard technology used in zebrafish. MO's are synthetic molecules similar to DNA but possess

a morpholine backbone instead of a deoxyribose backbone and bind to complementary sequences of RNA. When injected into embryos at the one cell stage, they transiently inhibit ("knock down") the target gene and effects can typically last up to 4 dpf. MO's are the most widely used antisense knockdown tool in zebrafish and are frequently used to accelerate gene discovery, as they are less time consuming than creating a mutant line (Bill et al., 2009). Permanent, targeted gene editing can also be performed in the zebrafish model by techniques, such as Zinc Finger Endonucleases (Foley et al., 2009), TALENs (Auer & Bene, 2014), and CRISPR/Cas9 (Prykhozhij et al., 2015). **Figure 1.7** displays retinal whole mounts in adult WT and *fzd4*$^{-/-}$ zebrafish. A *fzd4*$^{-/-}$ mutant zebrafish was generated in the Berman Zebrafish Lab (S. Prykhozhij) by transcription activator-like effector nuclease (TALEN) technology. These adult *fzd4*$^{-/-}$ zebrafish exhibit a FEVR-like phenotype displaying areas of vascular disorganization and hyper-vascularization (**Figure 1.7**, red arrow), illustrating the successful use of zebrafish to study FEVR. Therefore, it is likely that this mutant line could be utilized for a high throughput drug screen if a FEVR like phenotype is also displayed during the larval stages.

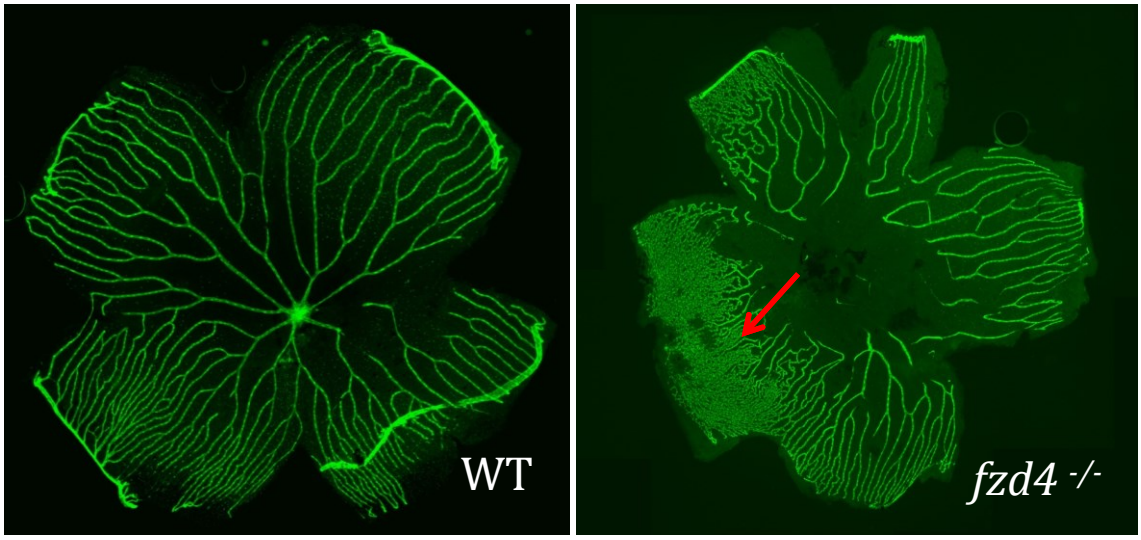

Figure 1.7. Retinal whole mounts in adult *fzd4* mutant zebrafish display a FEVR-like phenotype.

A wild type retinal whole mount on the right depicts an overall organized and non-pathological retinal network. However, in *fzd4* $^{-/-}$ zebrafish, there appears to be a robust difference in vascular organization highlighted by the red arrow.
(Courtesy of Sergey Prykhozhij).

1.9 Drug screens utilizing zebrafish

Due to the availability of large numbers of embryos, zebrafish can be used to screen thousands of chemicals simultaneously and be analyzed for phenotypic changes from the single cell stage up to larval stages (Zon & Peterson, 2005). Due to their small size (up to 4 mm in length by 5 dpf), zebrafish larvae can be placed in the wells of a 96 well culture plate and treated with small volumes of compounds dissolved in their aqueous medium, which increases throughput and minimizes the amount of compound needed for initial screens (Nusslein-Volhard & Dahm, 2002; Kitambi et al., 2009). Small molecule screens have been carried out in zebrafish to identify chemicals affecting regeneration, metabolism, retinal angiogenesis, and embryogenesis (Mathew et al., 2007; Kitambi et al., 2009; Yu et al., 2008)

1.10 Hypothesis and rationale

Prior to my research, the TALEN *fzd4*$^{-/-}$ mutant zebrafish model was created to use as a model for these drug screens. In addition, the novel *CDH5* gene was discovered, so preliminary studies were carried out by knocking down *cdh5* in zebrafish via morpholino. I hypothesize first that *cdh5* and *fzd4* loss of function in zebrafish will recapitulate a FEVR-like phenotype in the larval stage, allowing this model to be utilized for a preliminary drug screen in an attempt to reverse the underlying vascular pathology in FEVR. Secondly, I predict that treatment of both zebrafish models with S1PR2 antagonists will rescue or improve the FEVR-like phenotype in the zebrafish retina. It is possible that if S1PR2, an inhibitor of vascular development, is blocked by an antagonist

the vascular disorganization found in the zebrafish FEVR models could recover or improve.

The objectives were to 1) characterize the phenotype found in zebrafish lacking *fzd4* (a known FEVR gene) via TALEN technology (a model previously generated) and *cdh5* (a novel FEVR gene) expression via morpholino knockdown and, 2) depending on the early characteristics of the disease in these two models, identify the model with the most easily and reliably quantifiable characteristic at the larval stage to 3) validate the S1PR2 receptor as a druggable target to treat the underlying pathology in our zebrafish FEVR model organism. Furthermore, we want to carry out a preliminary small molecule drug screen in a higher throughput manner as compared to drug screens in FEVR mouse models. This will aid in determining which compound targets to pursue in mouse model studies of FEVR and possible human clinical trials in the future. We use the *cdh5* knockdown zebrafish as an in-vivo model to mimic FEVR in order to measure the phenotypic changes in the zebrafish eyes induced by the selected S1PR2 antagonists in **Table 1.2**.

We used multiple eye size parameters as a surrogate to analyzing retinal vasculature to quantify the phenotypic changes induced by the small molecules, in order to increase the efficiency of the drug screening method. We also carried out a qualitative assessment of retinal vasculature in the zebrafish *cdh5* knockdown model exposed to the predicted S1PR2 antagonists to determine if there were any effective drug targets in the list of 15 compounds predicted to antagonize S1PR2.

CHAPTER 2: MATERIALS & METHODS

2.1 Zebrafish husbandry and housing

Adult zebrafish (*Danio rerio*) were kept at 28.5°C under a standard 14 hour:10 hour light:dark schedule (Westerfield, 2000), and were fed Gemma-Micro 300 (Skretting, Vancouver, BC, Canada) once daily. Adult zebrafish were housed in a recirculating commercial zebrafish system (Pentair, Apopka, FL). Zebrafish experiments were approved by the Dalhousie University Committee of Laboratory Animals (UCLA), under protocol #15-134.

Embryos were collected (f*zd4*$^{-/-}$ transgenic line and *Tg(flia1a:EGFP)* followed by *cdh5* MO injection) and grown up at 28.5°C in E3 embryo medium (5mM NaCl, 0.17 mM KCl, 0.33 mM $CaCl_2$, and 0.33 mM $MgSO_4$). Methylene Blue was added to E3 embryo medium to halt the growth of fungus ($1x10^{-5}$ [v/v]). Embryos were permitted to be kept in egg water for up to seven days in Petri dishes, prior to being transported to adult zebrafish tanks. In cases where pigmentation needed to be reduced, the egg water was supplemented with 0.003% (w/v) 1-phenyl-2-thiourea (PTU; Sigma-Aldrich, St. Louis, MO, USA). Embryos requiring early dechorionation were treated with a 10 mg/mL (100µL/1mL) stock of Pronase for approximately five minutes at 28°C.

2.2 Morpholino oligonucleotide (MO)

Morpholino oligonucleotides were purchased from Gene Tools LLC, Philomath, OR. The *cdh5* MO used blocked sites involved in splicing pre-mRNA (a splice blocking MO) (5'-TACAAGACCGTCTACCTTTCCAATC-3') (Montero-Balaguer et al., 2009). A mismatch *cdh5* MO was used as a control (5'-TAgAAcACgGTCTAgCTTTCgAATC-

3') where lower case letters represent base pairs which have been replaced to create the mismatch MO. MO's were diluted with sterile water to 0.3 mM concentrations and heated at 65°C for 10 minutes. Embryos were collected and pooled prior to injections. MO's were then suspended in 0.05% (w/v) phenol red to aid in visualization of the injected volumes into *tg*(*fli1a*:*EGFP*) zebrafish embryos at the 1-4 cell stage. Approximately 1-2 µL of MO was injected into the yolk sac of each embryo using a micro-capillary glass needle connected to a PLI-100A Pico-injector microinjection system (Harvard Apparatus, Holliston, MA). Embryos were maintained in 10 cm Petri dishes inside a 28°C incubator until phenotypic evaluation. Embryos were also screened for GFP expression in the vasculature and only those expressing GFP were used for experiments.

2.3 Zebrafish imaging

Fluorescent images (150X magnification) as well as screening to validate that embryos expressed GFP was carried out using a (Discovery.V20 stereo microscope) connected to a (Zeiss AxioCam 506 color camera) and recorded using Zen 2 pro software (v 2.0) (Carl Zeiss Microimaging, Oberkochen, Germany). Zebrafish *fzd4*$^{-/-}$ tail vasculature images were taken with a (Observer.Z1 microscope (10X objective)) connected to an (Zeiss AxioCam 506 color camera). The same image acquisition settings were used for each experiment. Zen Imaging Software was used to transfer and process all images. Methylcellulose (3% w/v) was used in some cases to aid in imaging as needed to properly position embryos. Zebrafish were also lightly anesthetized with 0.2% Tris-buffered tricaine prepared in E3 embryo medium for imaging.

Retinal whole mounts were visualized using Zeiss Axio Imager Z2 microscope (Carl Zeiss Microimaging GmbH, Gottingen, Germany) containing a digital stage and the MosaiX software program in Axiovision 4.8. All analyses were performed on images captured at 10X magnification with the same acquisition settings.

2.4 Toxicity curves

Zebrafish were exposed to compounds at 2 dpf up until 6 dpf (4 days of total exposure). Compounds from **Table 1.2** were prioritized in terms of the solubility of the compound in water (logSW) values due to the compounds being added to a water bath, to avoid issues with precipitation. The tool compound JTE-013, an S1PR2 antagonist, was also included in the preliminary drug screen to determine if it produced a measurable reversal of the phenotype in the *cdh5* morphants. Compounds from **Table 1.2** were purchased in powder form from ChemBridge Online Chemical Store (www.hit2lead.com). In 2 dpf zebrafish, toxicity curves were carried out with JTE-013, methyl (2S) - [(6-isopropyl-1-methyl-1H-pyrazolo[3,4-d]pyrimidin-4-yl) amino] (phenyl) acetate "compound 1", N-[(benzylamino) carbonyl]-2,6-dichloro-4-methylnicotinamide "compound 2", N-[1-(1H-benzimidazol-2-yl) ethyl]-1,3,6-trimethyl-1H-pyrazolo [3,4-d] pyrimidin-4-amine "compound 3", and 2,6-dichloro-N-{[(2,5-dichlorophenyl) amino] carbonyl}-4-methylnicotinamide "compound 4". A stock solution of 10 mM in 2% DMSO of each compound was first made and serial dilutions were carried out to make the appropriate concentrations. For JTE-013, the concentrations used were 0, 6.25, 12.5, 25, 50, 100, and 200 μM. For compounds 1-4, the concentrations used were 0, 5, 10, 15, 20, 50, and 100 μM. To determine the toxicity of all compounds, *Tg*(*fli1a*:*EGFP*) zebrafish embryos at 2 dpf were placed individually into the wells of a 96 well plate in

PTU egg water with 2% dimethylsulfoxide DMSO added. A total of 18 larvae were used per group. Next, 100 µL of the compound solution was added for a total of 200 µL of solution per well. The presence or absence of zebrafish death was monitored over the next four days post treatment (dpt) and tallied. All toxicity curves were repeated a minimum of two times to determine the max tolerated dose (MTD) using the % survival averages between the replicates. The MTD was determined by the concentration at which 80% (+/- 5%) of the zebrafish survived by the endpoint. The MTD-50, one half the MTD concentration, was the first compound dosage applied to the zebrafish in the preliminary drug screen.

2.5 Preliminary drug screen

The *cdh5* morphant zebrafish were used for the preliminary drug screens. We used the zebrafish eye size as a parameter (vertical outer length, horizontal outer length, vertical inner length, horizontal inner length, outer eye area (**Figure 1.6 B**, red arrow), inner eye area (**Figure 1.6 B**, blue arrow)) to gauge improvements in the retinal vasculature phenotype. In addition, a qualitative relative vascular scale was used to correlate a change in eye size with a corresponding change in severity of retinal vasculature following treatment with compounds (described below). *Tg(fli1a:EGFP)* zebrafish injected with a *cdh5* mismatch MO, both treated (with the MTD-50 for the corresponding compound) and untreated were used as controls. Initially, µM rather than nM concentrations of JTE-013 were applied to a water bath containing the *cdh5* morphants in a similar method as described here. A decision was made to focus the preliminary drug screen on lower compound doses, in the nM range as during preliminary analysis there was no noticeable phenotypic change with higher µM JTE-013

concentrations. Although the tool compound JTE-013 is specific to S1PR2, it still possesses an affinity for the opposing S1PR's, S1PR1 and 3. JTE-013 does not inhibit S1PR1 up to a concentration of 10 μM and has a reported weak 4.2% inhibition of S1PR3 at 10 μM in human umbilical vein endothelial cells (HUVEC) (Osada et al., 2002; Parill et al., 2004). Thus at higher doses it could potentially be targeting the opposing S1PR1 and 3, resulting in an unwanted drug response. We believe this phenomenon may have been seen at μM doses.

Increasing doses of each compound (20, 50, 100, 500, and 1000 nM) were added to the wells of a 96-well containing *cdh5* morphant larvae at 2 dpf and the phenotype was assessed at 4 dpf by analyzing the JPEG photographs of the zebrafish eyes. Ten zebrafish larvae were treated with each dose of compound. ImageJ eye size analyses was carried out on JPEG images of the fish eyes in each group, in **Figure 2.1**, highlighted by the yellow outlines. ImageJ measured what was defined as the "vertical outer length", "horizontal outer length", "vertical inner length", "horizontal inner length", "area whole eye", and "area inner eye". All of these measurements are represented by arbitrary units (**Figure 2.1**). ImageJ analyses measuring eye size parameters for JTE-013, compound 1, and compound 2 was also carried out blinded experimenters to validate that the same trends were observed.

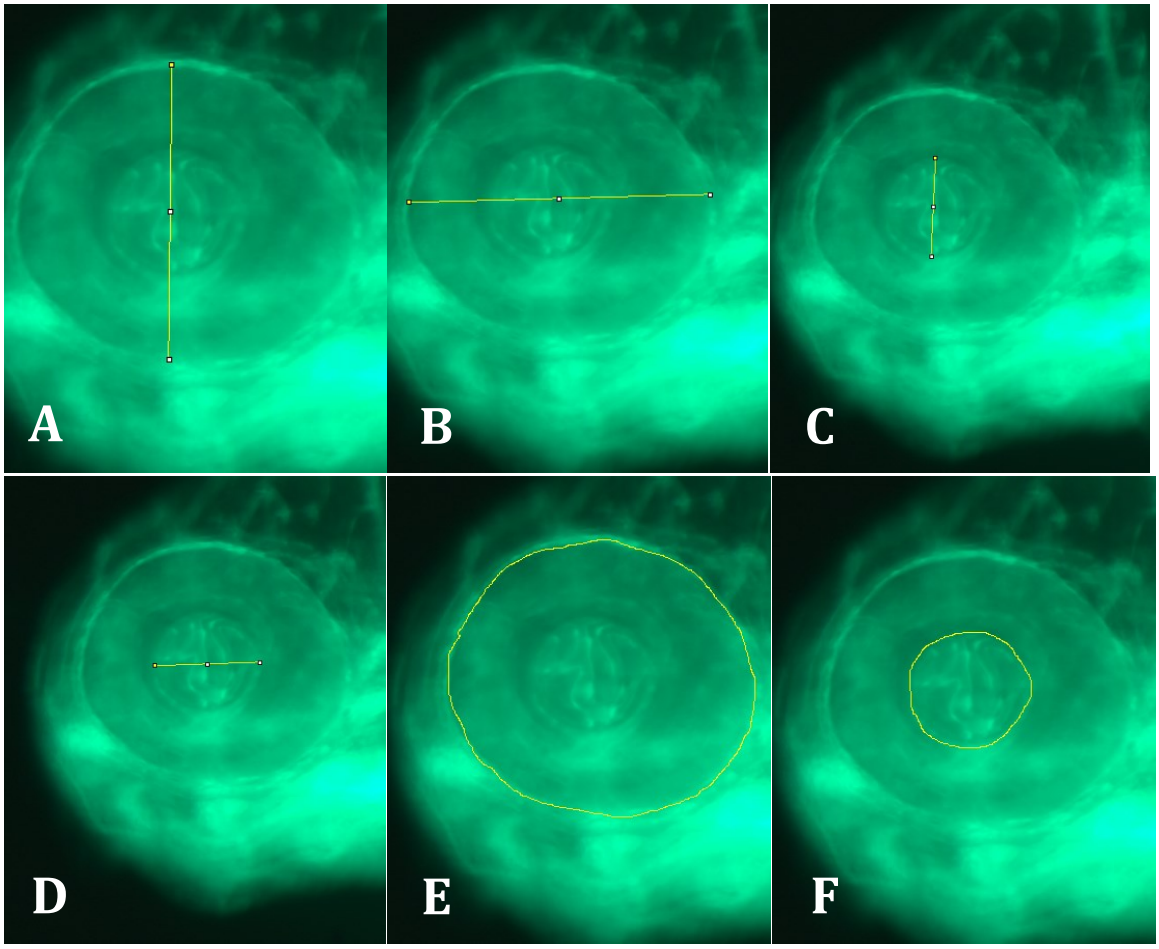

Figure 2.1. Zebrafish eyes at 4 dpf displaying the six parameters used to measure eye size.

Zebrafish (*Tg*(*fli1a*:*EGFP*)) were used in a preliminary drug screen where chemical compounds were added at 2 dpf and fluorescent photographs of the eyes were captured at 4 dpf as an outcome measure. Eye size was measured using ImageJ on JPEG files with six different parameters depicted by yellow lines, A-vertical outer length, B- horizontal outer length, C- vertical inner length, D- horizontal inner length, E-area whole eye, F-area inner eye. A similar method was also used to determine if there was an eye size difference between *fzd4*$^{-/-}$ zebrafish and wildtype *Tg*(*fli1a*:*EGFP)* zebrafish.

2.6 Qualitative retinal vascular scale

To determine if a change in eye size was correlated with the severity in retinal vasculature in the *cdh5* morphant fish, a subjective qualitative scale ranging from A-C was used. Similar qualitative methods to evaluate zebrafish vasculature have been used successfully in the past (Wu et al., 2015). A representative image from each of the categories are displayed in **Figure 2.2** where category (A) represents the least severe retinal vasculature and shares similarities to a WT zebrafish retina, category (C) represents the point on the scale with the most severe retinal vasculature where the retina consists of a circular stalk of vasculature, and (B) represents a severity of retinal vasculature between (A) and (C) whereby the retina still shows vessels branching but they appear more disorganized and appear to have their vessel integrity compromised. These characteristics areas are highlighted by red arrows in **Figure 2.2**. The average number of fish placed in each category between two blinded experimenters was calculated.

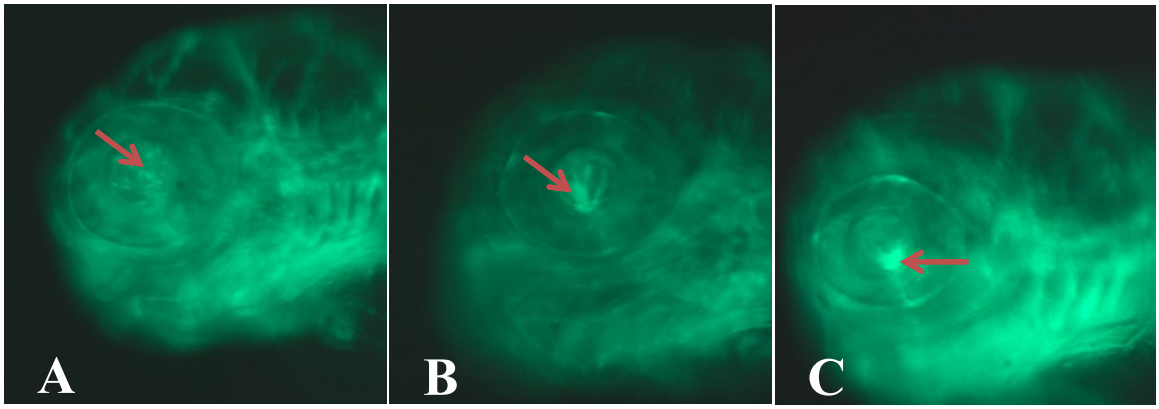

Figure 2.2. Representative images used in a qualitative retinal vascular scale.

Zebrafish (*cdh5* morphants, *Tg*(*fli1a*:*EGFP*)) at 4 dpf from each of the three JTE-013 drug screen replicates were subjectively analyzed to see if the severity of their retinal vasculature correlated with changes in eye size induced by compound treatment. Images (A-C) are representative photos used by blinded experimenters to categorize a vascular scale where (A) represents the least severe retinal vasculature and has similarities to a WT zebrafish retina, (C) represents the point on the scale with the most severe retinal vasculature where the retina consists of a circular stalk of vasculature, and (B) represents intermediate retinal vasculature between (A) and (C) whereby the retina still shows vessels branching but they appear more disorganized and appear to have their vessel integrity compromised. These areas of interest are indicated by red arrows.

2.7 Zebrafish *fzd4*$^{-/-}$ transgenic line construction & genotyping

Previously, Dr. Sergey Prykhozhij of the Berman Zebrafish Laboratory designed a pair of TALENs to target the *fzd4* gene in zebrafish to utilize in this research. In brief, zebrafish eggs were injected with *fzd4* TALEN mRNA's, grown up to 3 dpf and genomic DNA was extracted. Through PCR amplification and enzymatic digestion, it was confirmed that mutations were induced by the *fzd4* TALEN proteins. An insertion mutation of ten nucleotides successfully disrupted the reading frame of the *fzd4* gene. Finally, batches of the injected zebrafish embryos were raised to adulthood and the first generation was screened for founders. Those founders carrying the mutation were mated with *Tg*(*fli1a*:*EGFP*) zebrafish and raised to adulthood. Pairs of *fzd4* heterozygotes also expressing the GFP trangene were mated to produce 1/4 homozygotes (*fzd4*$^{-/-}$), which were used as breeding stock for all subsequent *fzd4* experiments and to maintain the *fzd4*$^{-/-}$ *line.*

2.8 *fzd4* $^{-/-}$ eye size analyses

Mutant *fzd4*$^{-/-}$ zebrafish were analyzed thoroughly at 3-7 dpf for any gross observable phenotype and in particular, the tail and retina were closely analyzed for any vascular abnormalities. Eye size was also analyzed between *fzd4*$^{-/-}$ zebrafish and wildtype *Tg*(*fli1a*:*EGFP*) zebrafish. Fluorescent JPEG images were used in accordance with ImageJ software to compare six different eye size parameters, as depicted in **Figure 2.1** and was similar to the preliminary drug screen eye size analysis above (section 2.5) (Schindelin et al., 2012).

2.9 *fzd4* $^{-/-}$ retinal whole mounts

Retinal whole mounts were isolated from both one month and three month old *fzd4* mutant zebrafish (Mike Ngo, Dalhousie University). One month old retinal whole mounts were taken from *fzd4* $^{-/-}$ zebrafish as well as wildtype *Tg*(*fli1a*:*EGFP*) zebrafish. For three month old zebrafish, retinal mounts were taken from *fzd4*$^{-/-}$ zebrafish, with and without JTE-013 treatment, as well as wildtype *Tg*(*fli1a*:*EGFP*) zebrafish, with and without JTE-013 treatment. A concentration of 50 nM JTE-013 was used for the compound treatment. As soon as possible after fertilization (one cell stage), 50 nM JTE-013 in E3 embryo medium with 2% dimethlysulfoxide (DMSO) was added to 10 cm Petri dishes up until 5 dpf then subsequently transferred to standard isolated adult housing tanks in regular water without any compound application. The JTE-013 compound treatment was replaced daily for the first five days following fertilization and embryos were incubated at 28°C.

At the appropriate time point, zebrafish at one month (no treatment) and three months (JTE-013 treatment) were overdosed with 0.2% Tris-buffered tricaine prepared in E3 embryo medium and eyes were carefully extracted using forceps and immediately placed into 4% paraformaldehyde (PFA) and left overnight for approximately 24 hours at 4°C in an Eppendorf tube. Both eyes were taken from each fish and kept separately. Retinas were washed three times with a phosphate buffered saline containing 0.1% Triton X-100 and each eye was flat mounted onto glass microscope slides (Fluoromont-G Sigma-Aldrich).

2.10 Statistical analyses

Statistical tests (unpaired t-test) for *fzd4*$^{-/-}$ eye size analyses were carried out using GraphPad Prism Software (GraphPad Software, Inc., La Jolla, CA, USA). Statistical analyses for drug screen eye size parameters on *cdh5* morphant zebrafish were carried out at the IWK Health Centre, Halifax, NS, CA with the help of the Perinatal Epidemiology Research Unit, Department of Pediatrics (Bryan Maguire). R software (2016) was utilized. A multivariate analysis of variance (MANOVA) was used to determine if eye size is statistically significant when all 6 measured parameters were taken into account. Furthermore, a general linearized model followed by a Welch Two Sample t-test was used to investigate JTE-013 and compound 1 with regards to one specific eye parameter, "area inner eye". P-values less than 0.05 were considered significant.

CHAPTER 3: RESULTS

3.1 *cdh5* morphants display a robust decrease in retinal vasculature

A MO targeting zebrafish *cdh5* in was injected at the one cell stage to determine if this morphant could be used to model FEVR and subsequent preliminary drug screens. There were no adverse phenotypes following injection of the *cdh5* mismatch MO (**Figure 3.1 A**). Following *cdh5* MO injection into *Tg(fli1a:EGFP)* zebrafish, a robust retinal phenotype was observed. Approximately 80% of injected embryos displayed the phenotype depicted in (**Figure 3.1 B**). Approximately 200 embryos were injected with the *cdh5* MO and this was repeated at least three different occasions. Retinal vasculature in *cdh5* morphants appears greatly reduced, with little to no branching of retinal vessels leaving a single vascular stalk. Eye size is noticeably smaller in morphants with an appreciable amount of edema around the eye as well as the heart was noted. The phenotype was not present until 4 dpf, with the exception of a small number of morphants (~25%) displaying some cardiac edema at 3 dpf.

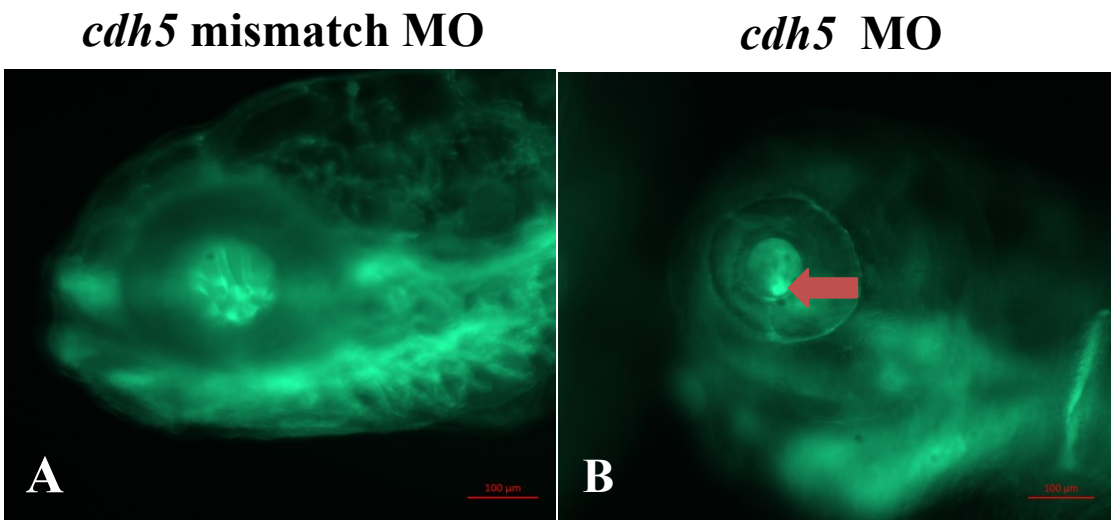

Figure 3.1. Zebrafish at 4 dpf injected with *cdh5* MO at the one cell stage display a robust decrease in retinal vasculature.

Approximately ~80% of *cdh5* morphants have retinal vasculature appearing as a single vascular stalk lacking vessels (B, red arrow) and have smaller eye size at 4 dpf.

3.2 Toxicity curves and MTD

Toxicity curves for the following compounds were successfully carried out a minimum of two times: JTE-013, compound 1, 2, 3, and 4. Some precipitation of the compounds was noted at higher doses during serial dilutions but these were not utilized in these curves. The MTD and MTD-50, respectively, for each of the compounds are as follows (**Figures 3.2-3.6**): JTE-013- 10μM, 5μM; compound 1- 10μM, 5μM; compound 2- 15μM, 7.5 μM, compound 3- 10μM, 5μM, and compound 4- 20μM, 10μM.

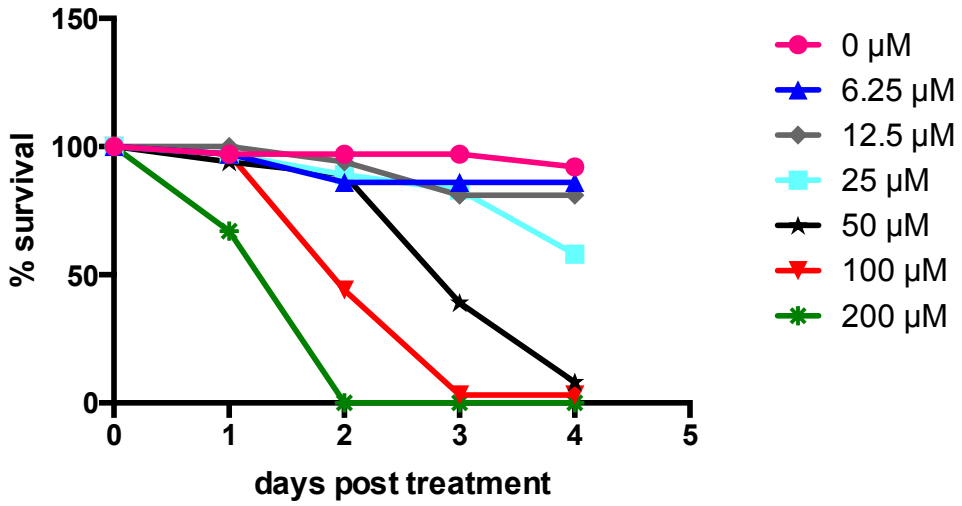

Figure 3.2. Toxicity curve for JTE-013 with an MTD of 12.5 µM.

n=18 zebrafish for each concentration.

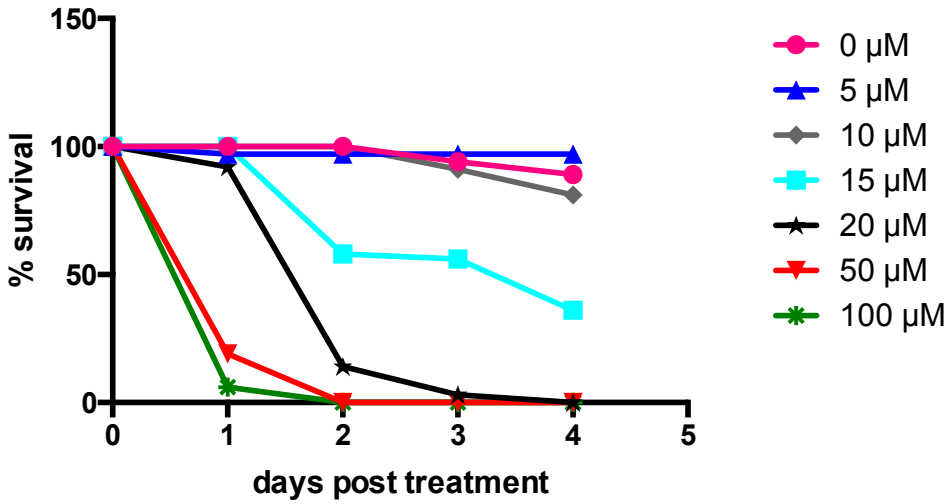

Figure 3.3. Toxicity curve for compound 1 with an MTD of 10 µM.

n=18 zebrafish for each concentration.

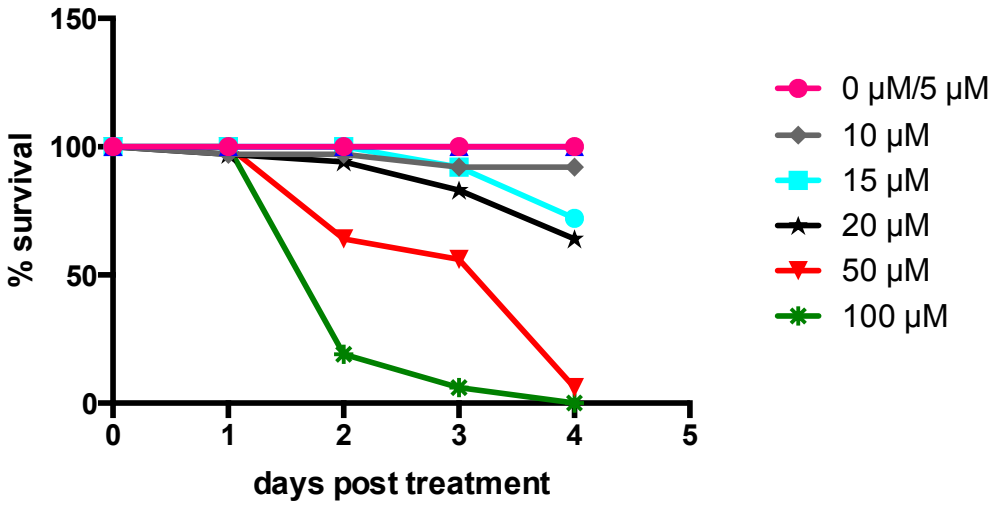

Figure 3.4. Toxicity curve for compound 2 with an MTD of 15 µM.

n=18 zebrafish for each concentration.

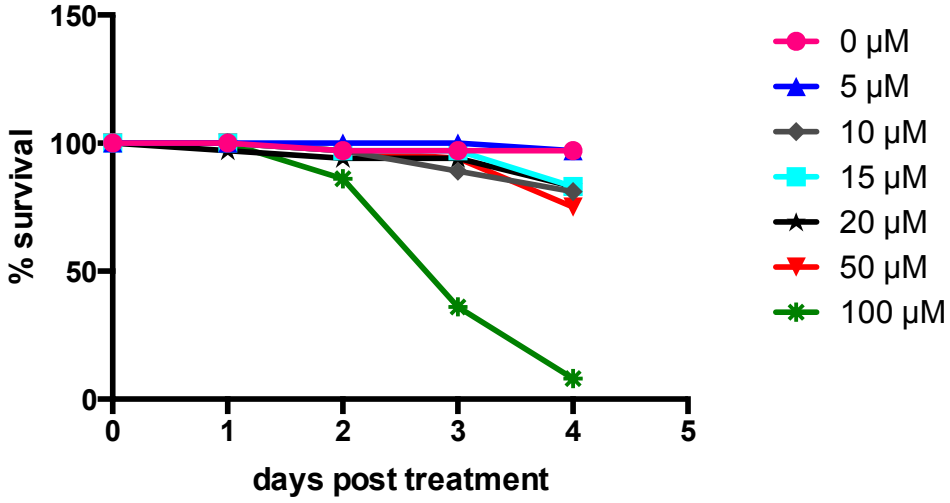

Figure 3.5. Toxicity curve for compound 3 with an MTD of 10 µM.

n=18 zebrafish for each concentration.

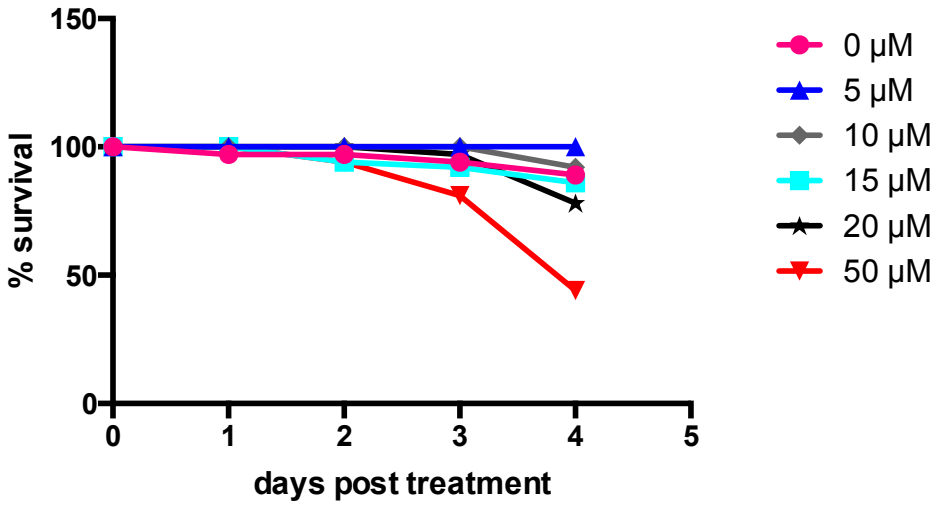

Figure 3.6. Toxicity curve for compound 4 with an MTD of 20 µM.

n=18 zebrafish for each concentration.

3.3 Preliminary drug screen shows JTE-013 & compound 1 significantly affect "area inner eye"

Statistics were carried out for JTE-013, compound 1, and compound 2 using data acquired from ImageJ analysis of the 6 eye size parameters. This data is currently unavailable for compounds 3 and 4 and only toxicity curves for them were included in this study. There were no significant changes to eye size when each compound was added to the mismatch *cdh5* morphant group (at the corresponding MTD-50 concentration). For all untreated experimental groups, all 6 measured eye size parameters (vertical outer length, horizontal outer length, vertical inner length, horizontal inner length, area whole eye, area inner eye (**Figure 2.1**)) in *cdh5* morphants were significantly different from that of the *cdh5* mismatch morphants (control group), indicating the gene knockdown alone had an effect on these eye size parameters (p-value <0.05). When all six eye size parameters are analyzed together, none of the tested compounds had a significant effect (MANOVA).

For JTE-013, when each eye size parameter was statistically analyzed separately and compared to untreated *cdh5* morphants, the "area inner eye" parameter had a p-value of 0.03. All other parameters had p-values above 0.05. This prompted further investigation into "area inner eye" specifically. **Figure 3.7** shows the data for "area inner eye" only, depicting that at concentrations of 20 nM (p-value= 0.02) and 50 nM (p-value= 0.004), "area of inner eye" seems to improve significantly compared to untreated cdh5 morphants (using general linearized model and Welch Two Sample t-test).

For compound 1, when each eye size parameter was statistically analyzed separately and compared to untreated *cdh5* morphants, the "area inner eye" parameter had a p-value of 0.02 prompting a similar investigation to that of JTE-013. **Figure 3.8**

shows data for “area inner eye” only, depicting that at concentrations of 20 nM (p-value= 0.03) “area inner eye” seems to significantly affect eye size compared to untreated *cdh5* morphants (using a general linearized model). However, upon closer evaluation of statistical data, it appears that at 20 nM concentrations of compound 1, this group had a lower mean compared to the untreated group. Thus, compound 1 significantly made “area inner eye” smaller.

Compound 2 did not improve eye size (p-values > 0.05, MANOVA) **(Figure 3.9)**.

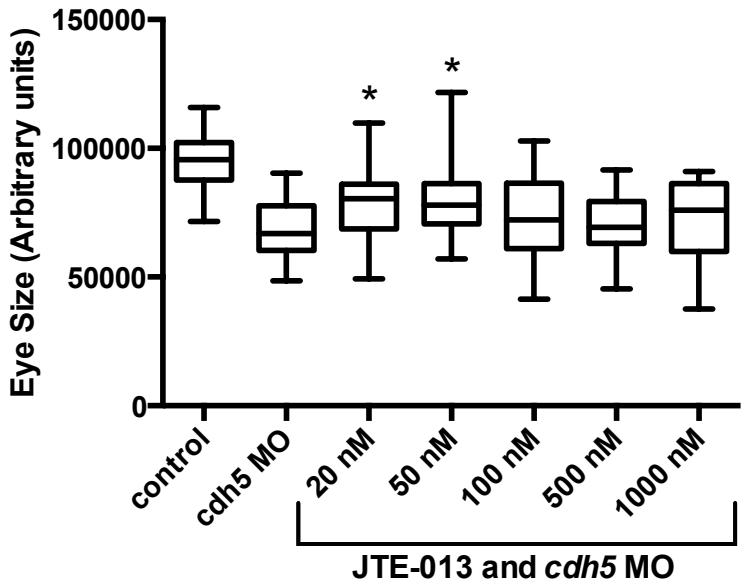

Figure 3.7. JTE-013 significantly improves "area inner eye" in *cdh5* morphants in a dose dependent manner.

Control groups are zebrafish injected with a mismatch *cdh5* MO. At concentrations of 20 nM (p-value= 0.02) and 50 nM (p-value= 0.004) of JTE-013 "area inner eye" significantly improves compared to the untreated morphant group (*cdh5* MO). Significance is indicated by an asterisk. The horizontal line in each box represents the median. The box extends from the 25th to 75th percentiles. n=10 for each concentration.

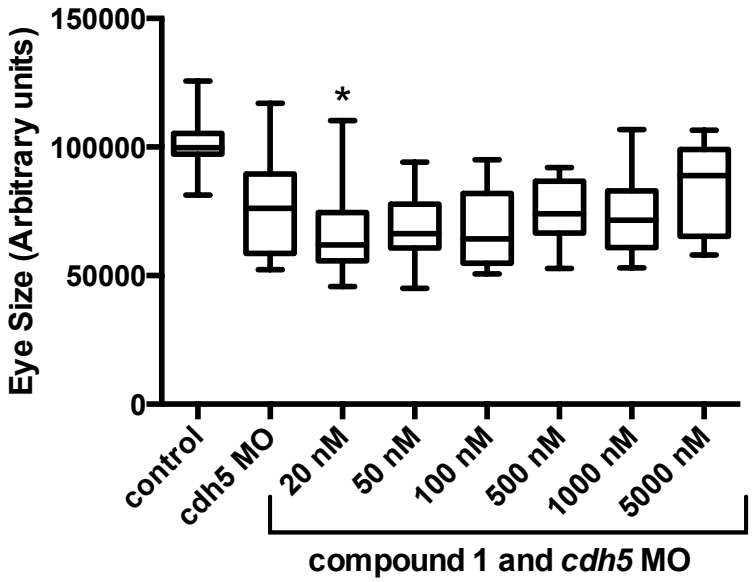

Figure 3.8. Compound 1 significantly decreases "area inner eye" in *cdh5* morphants.

Control groups are zebrafish injected with a mismatch *cdh5* MO. At concentrations of 20 (p-value= 0.03) of compound 1 "area inner eye" significantly decreases compared to the untreated morphant group (*cdh5* MO) therefore making "area inner eye" smaller. Significance is indicated by an asterisk. The horizontal line in box represents the median. The box extends from the 25th to 75th percentiles. n=10 for each concentration.

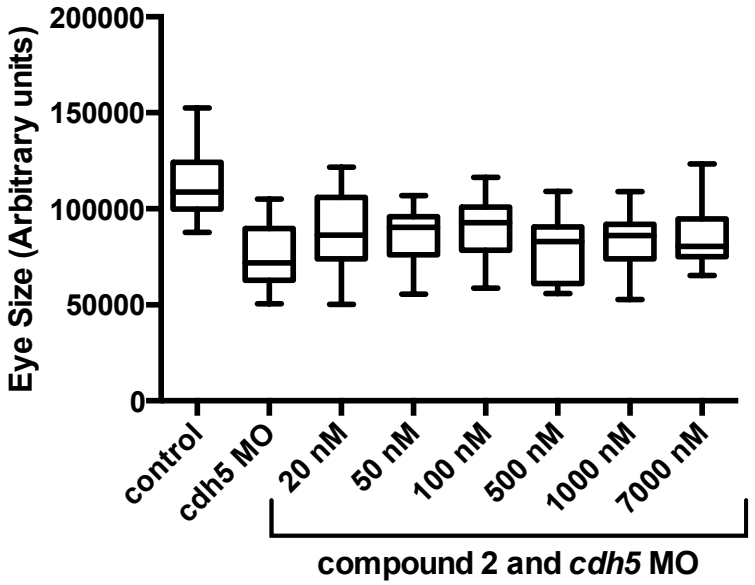

Figure 3.9. Compound 2 has no effect on eye size in *cdh5* morphants.

Control groups are zebrafish injected with a mismatch *cdh5* MO. At the above concentrations of compound 2, "area inner eye" does not significantly improve compared to the untreated morphant group. The horizontal line in each box represents the median. The box extends from the 25th to 75th percentiles. All p-values for all compound 2 concentrations were above 0.05. n=10 for each concentration.

3.4 Qualitative retinal vascular scale shows an improvement in "area inner eye" is associated with improved retinal vasculature

The improvement in eye size upon addition of JTE-013 to *cdh5* morphants at concentrations of 20 nM and 50 nM also appears to improve retinal vasculature (**Figure 3.10**). The 20 nM and 50 nM groups had more morphants in category (A), the category which looks most similar to WT zebrafish retinal vasculature, compared to the other treatment groups as well as the untreated *cdh5* morphant group. The number (averaged) of zebrafish in category (C) is as follows: *cdh5* mismatch MO (control)=1.5, *cdh5* MO untreated= 18.5, 20 nM= 10.5, 50 nM= 12.5, 100 nM= 15.5, 500 nM= 14, 1000 nM= 18.

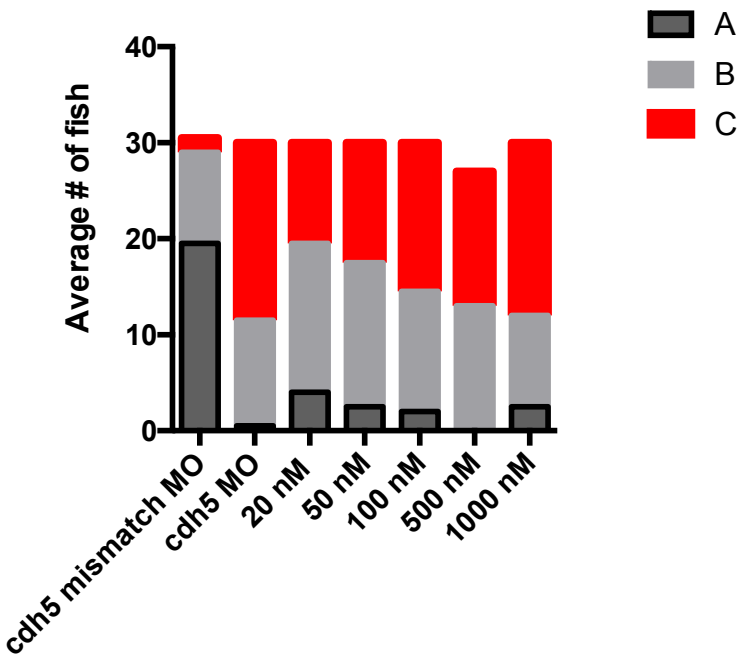

Figure 3.10. Retinal vasculature appears to be associated with improvements in "area inner eye".

Data represents pooled data from three separate JTE-013 preliminary drug screens. Categories: (A)- represents the least severe retinal vasculature and has similarities to a WT zebrafish retina, image (C) represents the point on the scale with the most severe retinal vasculature where the retina consists of a circular stalk of vasculature. (B) represents a severity of retinal vasculature between (A) and (C) whereby the retina still shows vessels branching but they appear more disorganized and appear to have their vessel integrity compromised. n=30 for each concentration (some death in the 500 nM concentration).

3.5 *fzd4*$^{-/-}$ mutants show no difference in eye size

The *fzd4*$^{-/-}$ mutant zebrafish were analyzed under a microscope to determine a larval phenotype that could be utilized in a drug screen. *fzd4*$^{-/-}$ phenotypic differences between WT *Tg(fli1a::EGFP)* were not observed at 2-7 dpf. There was no gross observable phenotype in the retina (**Figure 3.11**, A and B, white arrows) and thus is not useful for a high throughput preliminary drug screen. Tail inter-segmental vessels appeared organized and healthy (**Figure 3.11**, C and D, white arrows). No obvious signs of cardiac edema were present. No difference in eye size was observed between *fzd4*$^{-/-}$ mutant zebrafish and WT *Tg*(*fli1a*:*EGFP)* zebrafish at 4 dpf (considering the six eye size parameters measured) (**Figure 3.12** A-F). Error bars indicate standard error of the mean (SEM, n=10).

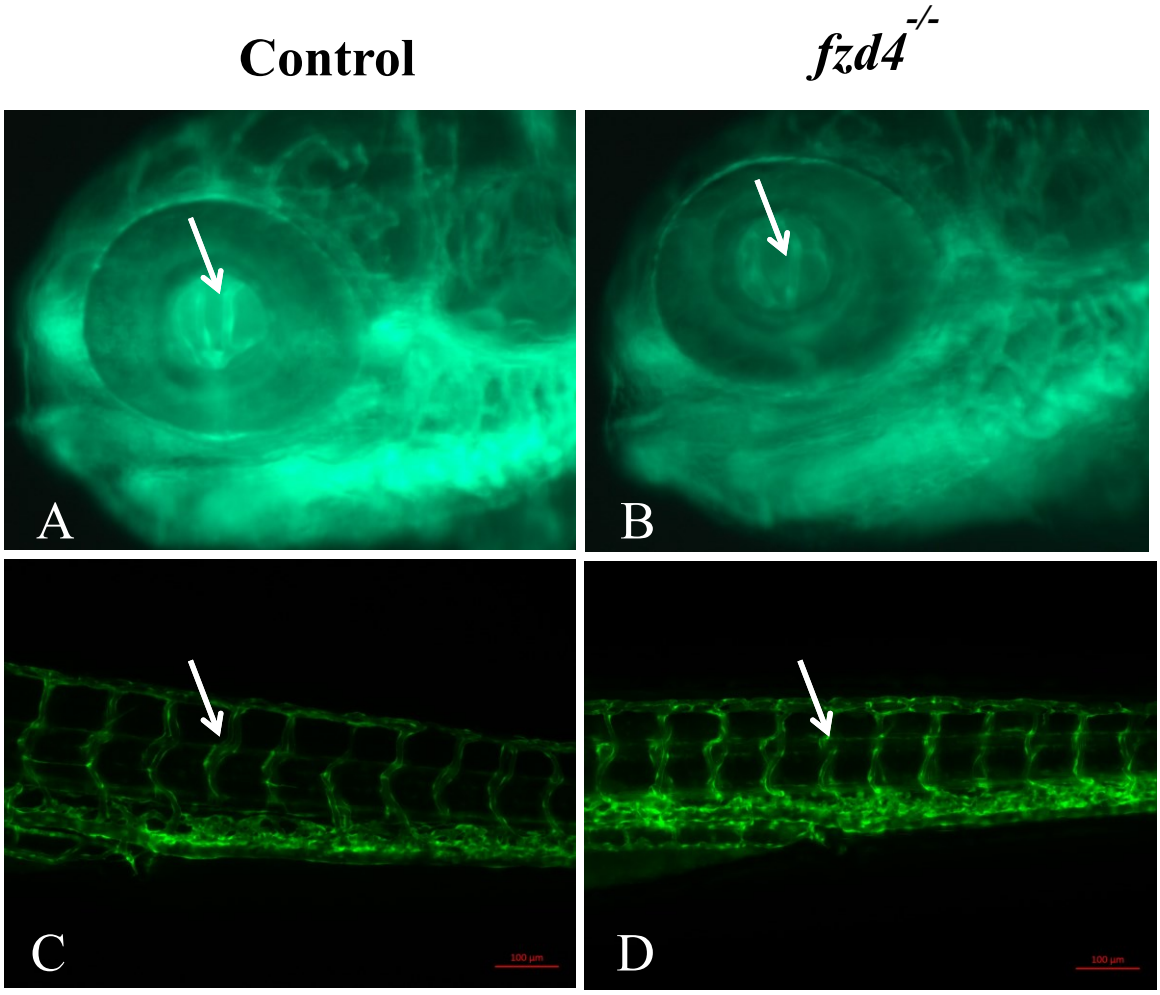

Figure 3.11. WT and *fzd4*$^{-/-}$ *Tg(fli1a:EGFP)* zebrafish display organized retinal and tail vasculature at 4 dpf.

Control WT *Tg(fli1a:EGFP)* as well as *fzd4*$^{-/-}$ mutant zebrafish at 4 dpf display normal vasculature. A- white arrow highlights organized retinal vasculature in a control zebrafish. B- white arrow highlights organized retinal vasculature in *fzd4*$^{-/-}$ mutants. No obvious signs of avascular or hyper-vascular areas are present. C and D- white arrows indicate a normal inter-segmental vessel in the zebrafish tail vasculature in control and *fzd4*$^{-/-}$ mutants, respectively.

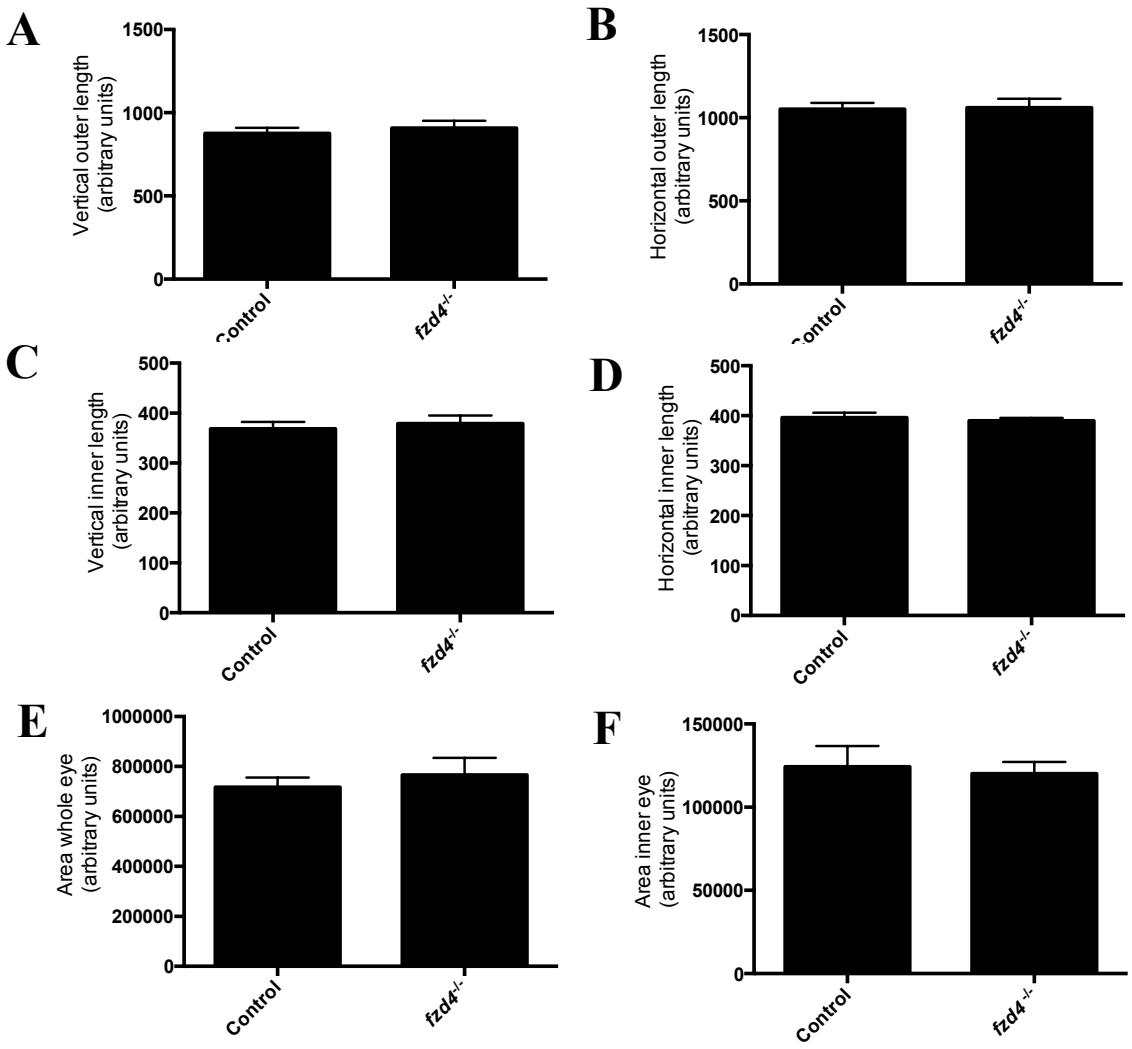

Figure 3.12. Eye size is not significantly different between WT and *fzd4*$^{-/-}$ *Tg(fli1a:EGFP)* zebrafish at 4dpf.

Six eye size parameters (**Figure 2.1**) were compared between control WT *Tg(fli1a::EGFP)* and *fzd4*$^{-/-}$ mutant zebrafish at 4 dpf. Eye size parameters were measured using ImageJ with arbitrary units and were insignificant compared to WT (unpaired t-test). Error bars represent standard error of the mean (SEM). n=10.

3.6 *fzd4*$^{-/-}$ retinal whole mounts are difficult to interpret

Retinal whole mounts of one month old WT and *fzd4*$^{-/-}$ mutant zebrafish were used to determine if a phenotype was present at a time point between three months, which was previously established (**Figure 1.6**), and the larval stage to establish the utility of this model in a high throughput drug screen (**Figure 3.13**). Representative images were chosen but unfortunately many retinal mounts suffered damage, complicating interpretation. The white arrow in **Figure 3.13** shows a hyper-vascular area that appears similar to the FEVR-like phenotype found in three-month old adult *fzd4*$^{-/-}$ mutant zebrafish (**Figure 1.6**). Adult zebrafish retinal whole mounts at three months that had been exposed to a 50 nM concentration of JTE-013, the S1PR2 antagonist, in a water bath up to 5 dpf, did not display recovery of the FEVR-like phenotype. Retinal whole mounts from each fish were kept separate so any differences between pairs of eyes could be observed (**Figure 3.14**). Again, representative images of a large sample (7 eyes for one month old zebrafish and 8 eyes/4 fish for the three month old samples) are shown and some mechanical damage is evident. If any compound effects exist, a more detailed method of quantification is needed in order to detect a difference.

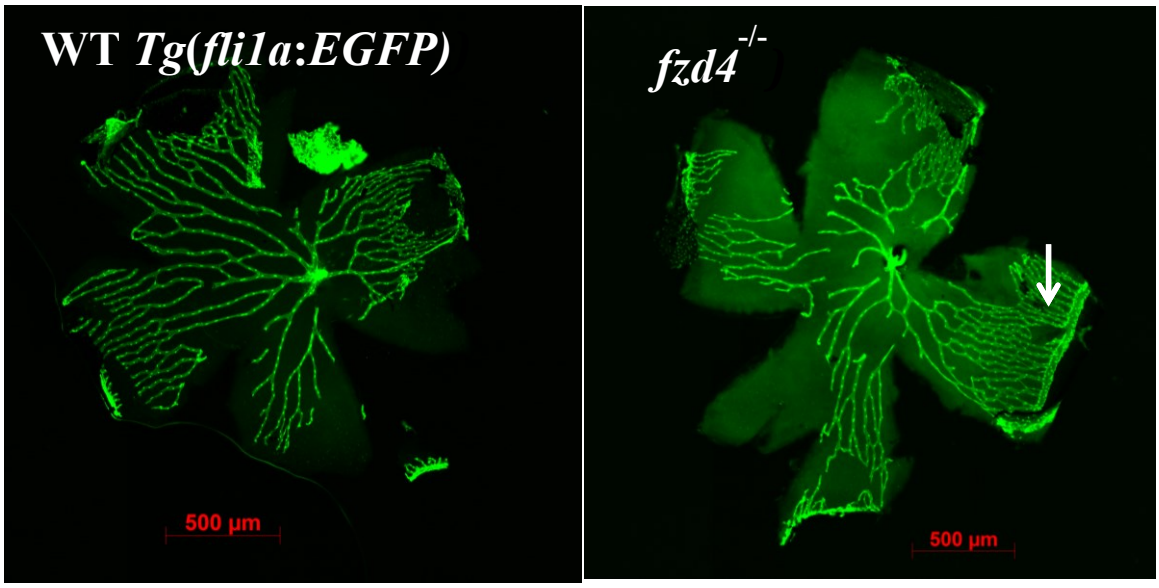

Figure 3.13. Representative images of one month old zebrafish retinal whole mounts are difficult to interpret.

Retinal whole mounts were taken of zebrafish at one month to determine if a FEVR-like phenotype was present at this time point. Both the WT *Tg(fli1a:EGFP)* and *fzd4*$^{-/-}$ mutant retinal whole mounts appear to possess mechanical damage and this was consistent throughout other samples. There appears to be hyper-sprouting in the periphery of *fzd4*$^{-/-}$ (white arrow) (n= 7 eyes).

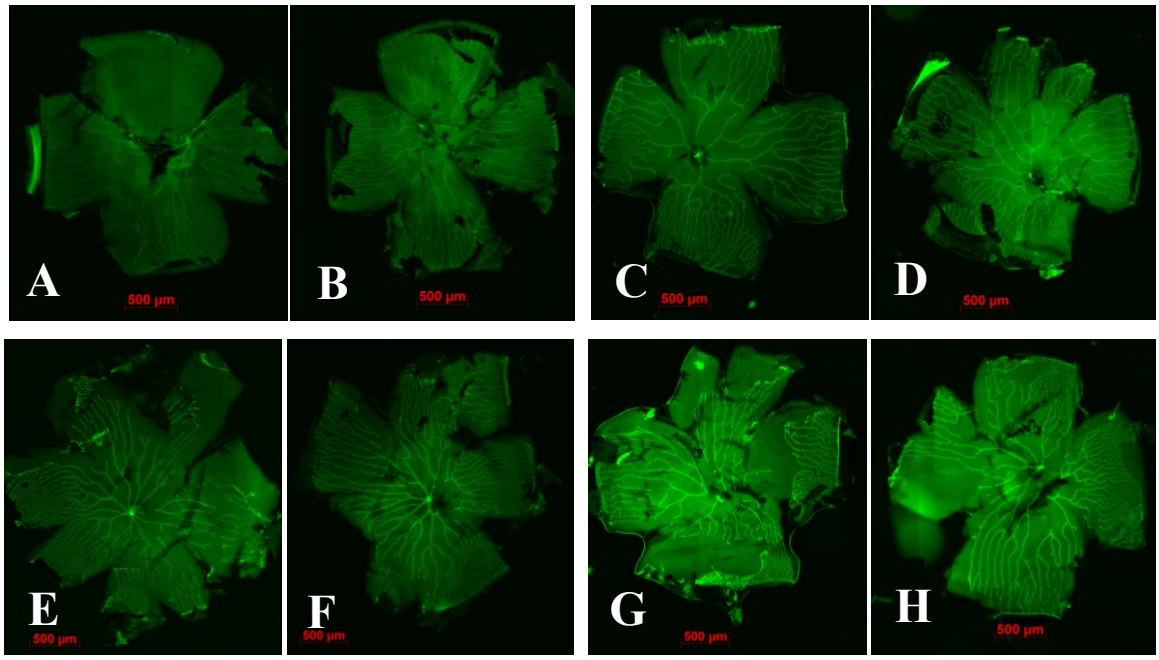

Figure 3.14. Adult *fzd4*$^{-/-}$ zebrafish retinal whole mounts at three months following JTE-013 treatment do not show any obvious signs of improvement.

Pairs of eyes were carefully enucleated from adult zebrafish at approximately three months of age and retinas were mounted to compare phenotypic retinal vascularization following JTE-013 treatment. WT *Tg(fli1a:EGFP)* and *fzd4*$^{-/-}$ zebrafish were treated with 50 nM JTE-013 for 5 dpf and subsequently raised to adulthood. Each row represents a pair of eyes from the same zebrafish. A and B- control WT *Tg(fli1a:EGFP)* zebrafish retinas untreated. C and D- control WT *Tg(fli1a:EGFP)* zebrafish retinas treated with JTE-013. E and F- *fzd4*$^{-/-}$ zebrafish retinas, untreated. G and H- *fzd4*$^{-/-}$ zebrafish retinas treated with JTE-013. n= 8 eyes/4 zebrafish.

CHAPTER 4: DISCUSSION

4.1 Summary

The main goal of this study was to identify new effective treatments for the childhood blinding disease FEVR in an efficient, cost effective manner. Several mouse models reveal impaired retinal vasculature following knockout of *Fzd4*, *Tspan12*, *Lrp5*, or *Ndp* FEVR genes (Luhmann et al., 2005; Xia et al., 2008; Xu et al., 2004; Gilmour, 2015).

The objectives were to 1) characterize the phenotype found in zebrafish lacking *fzd4* (a known FEVR gene) via TALEN technology and *cdh5* (a novel FEVR gene) expression via morpholino knockdown and, 2) depending on the early characteristics of the disease in these two models, identify the model with the most easily and reliably quantifiable characteristic at the larval stage to 3) validate the S1PR2 receptor as a druggable target to treat the underlying pathology in our zebrafish FEVR model organism.

We have demonstrated that zebrafish *cdh5* morphants exhibit a robust retinal vascular phenotype, which is easily observable at the larval stage, and that eye size parameters can be used as a measure of phenotypic rescue for a high throughput screen, with our current data set. We also show that JTE-013 has the ability to improve eye size in a significant manner in *cdh5* morphant zebrafish indicating S1PR2 could potentially be a successful therapeutic target.

4.2 *cdh5* morphants display a FEVR-like phenotype

To determine whether *CDH5,* a novel FEVR gene, could be genetically manipulated in zebrafish to mimic a FEVR-like phenotype, a morpholino targeting *cdh5* was injected. Zebrafish injected with *cdh5* MO displayed a robust retinal vascular phenotype (**Figure 3.1**) characterized by failure of progression of ocular vascularization beyond the primitive hyaloid vessel, with complete failure of vascular branching from the main stalk. This provides strong evidence for a role for *CDH5* in humans with FEVR (manuscript in preparation) in addition to providing a useful tool to evaluate the effects of novel therapeutics at a very early stage, thus enabling high throughput screening using zebrafish.

4.3 Eye size can potentially be used as a surrogate of retinal vascular disease

This study demonstrated that eye size may be an accurate predictor of severity of retinal vasculature. Using the six different eye size parameters as a measure of the influence of the compounds predicted to interact with S1PR2 allowed for maximization of time, as opposed to quantifying retinal vascular phenotype. There is no known technique that measures axial length (the distance from the surface of the cornea to the back of the eye) in zebrafish in a manner similar to A-scan ultrasound biometry in humans. Axial length could potentially be measured in zebrafish by using ImageJ analysis of larval eye images taken from a different angle than the images represented here. Although axial length was not specifically measured in this study, it is likely that axial length changes the eye size parameters and that measuring the other parameters such as diameter and circumference can reliably provide an alternative.

In humans, microphthalmia is frequently associated with conditions characterized by developmental retinal vascular insufficiency including ROP, PFV and FEVR (Hu et al., 2016; Goldberg, 1997; Robitaille et al., 2009). Several studies have shown a correlation between smaller eye size and severity of the retinal vascular pathology indicating that the pathological groups have an increased susceptibility to microphthalmia (Ouyang et al., 2015; Yang et al., 2013; Fledelius & Fledelius, 2012). Specifically, infants with ROP have been demonstrated to have shorter axial lengths and myopic refractive error from increased corneal steepness and anterior positioning of the lens that correlated with the degree of prematurity and low birth weight (Ouyang et al., 2015; Chen et al., 2010). One can hypothesize that zebrafish FEVR models may also possess these characteristics.

I was able to determine that zebrafish injected with *cdh5* morpholino also display evidence of microphthalmia. Zebrafish injected with *cdh5* MO displayed a retinal vascular phenotype and decrease in eye size which we uniquely quantified by measuring 6 different eye size parameters (**Figure 2.1**). The eye size parameter which was found to be significant, "area inner eye", likely corresponds to the lens area as depicted in **Figure 1.6 A** in the transverse section of the histological zebrafish eye**.** The variability of the morphant phenotype may be a reflection of the morpholino injections themselves, despite the same concentration loaded into each capillary needle, the dosage is likely variable, even though a similar-sized bolus is injected. Alternatively, the zebrafish may display phenotypic variability in the same manner seen in human FEVR patients regardless of morpholino dosage. Those zebrafish injected with the control mismatch *cdh5* MO did not display this variability. Despite this, we found that using eye size as a read out of severity

of retinal vasculature allowed for a more rapid analysis of the impact or effect of several compounds predicted to interact with S1PR2.

Finally, zebrafish were observed at the same time point and in a lab-controlled environment where all fish were exposed to the same conditions. However, it might be important to consider that only one eye from each fish was included in the drug screening quantitative analyses (except for the three month old zebrafish retinas treated with JTE-013 where pairs of eyes were observed, **Figure 3.14**). However, as FEVR is virtually always bilateral, the difference in eye size between the two eyes of the same zebrafish is not expected to vary significantly.

4.4 S1PR2 can successfully be targeted in *cdh5* morphant zebrafish

This study shows that targeting S1PR2 significantly improves eye size in our zebrafish FEVR model, specifically the parameter "area inner eye". JTE-013 significantly improved the "area inner eye" at concentrations of 20 nM and 50 nM. "Compound 1" had a significant effect on eye size at 20 nM concentrations but made the eyes of the *cdh5* morphants even smaller. "Compound 2" appeared to have an insignificant effect and these compounds will not move to mouse studies. It is important to note that the 15 compounds in **Table 1.2** are not JTE-013 analogues so it may not be surprising that "compound 1" had opposite effects on eye size as compared to JTE-013. There are two basic approaches to the theory of drug design, 1) structure based, and 2) ligand based (Hruby, 2002). The compounds tested here are based on the receptor structure of S1PR2. It is possible that "compound 1" caused off target effects such that it may have had agonistic effects on S1PR2 (stimulating the inhibitor of angiogenesis), or

alternatively, an antagonistic effect on S1PR1 and 3 (blocking the promotion of angiogenesis). The off target effects may not be limited to the S1P pathway and it is possible that compound 1 was stimulating or inhibiting some other intracellular signaling pathway that also regulates blood vessel development. These compounds were predicted by software to structurally fit the receptor, however this is not a guarantee that the compound will be active biologically. There is little information known about the pharmacokinetics of the compounds predicted to interact with S1PR2 tested in this study.

An additional value to identifying early the effects of compounds that are biologically active in our model is that it can help guide the development and choice of future compounds to be tested next. Consultation with a chemist to synthesize JTE-013 analogs (in addition to compounds predicted to interact with S1PR2) is currently underway in view of screening these new compounds using the *cdh5* zebrafish platform established here.

Due to the paucity of information regarding the properties of the new compounds, determining the MTD for each compound was utilized as a starting point. As more details are known about the compounds being screened, less time will need to be allocated to adjust effective concentrations. This leads to the ADME (absorption, distribution, metabolism, and excretion) concepts of drugs. As mentioned previously, JTE-013 is rapidly metabolized, preventing its effective use as a drug. Also, an ideal drug should also not be metabolized so slowly that it accumulates in tissues causing indirect consequences including toxicities. It is not known what the best developmental time point to add the compound to the water bath. It would be worthwhile adding the compounds of interest directly after fertilization and making comparisons to the results

we found after addition of each compound a 2 dpf. We found that 4 dpf was an ideal endpoint because at this developmental point the retinal vasculature is clearly visible to capture images on a microscope.

The specific parameter "area inner eye" is not currently measured in zebrafish as a research tool and can be used in high throughput screening of other candidate compounds to treat FEVR. When all six eye size parameters were statistically analyzed together, none of the compounds appeared to have a significant effect. This suggests that "area inner eye" is influenced to a greater extent compared to the other 5 parameters, when all parameters are analyzed simultaneously, the effects on the "area inner eye' are lost in the combined measures. As the early vascular events that lead to retina vessel development involve a hyaloid system that wraps around the lens in both humans and zebrafish, a plausible explanation for the increased susceptibility of the "area inner eye" is that disruption at that phase in development will influence measures directly at level of the lens to a greater extent and earlier on than the outer ocular structures.

Interestingly, Collin and colleagues (2013) used MO to knockdown *znf408*, a known FEVR gene in zebrafish, and discovered defects in the developing retina, specifically the dorsal, nasal, and ventral intraocular ring vessels, as well as trunk vasculature illustrating the utility of zebrafish in studying vascular disease. The vascular defects seen in *znf408* zebrafish morphants appear to be less dramatic than the retinal phenotype observed in *cdh5* morphants in our study. The intraocular ring vessels were not abnormal in the *fzd4*$^{-/-}$ mutant zebrafish (data not shown) but would be another part of the eye vasculature to be aware of when screening for phenotypes in other FEVR fish

models. The compounds used in this preliminary drug screen could easily be tested using a similar protocol in other zebrafish genetic models of FEVR.

To date, no other study has demonstrated a role for S1PR2 in the treatment of FEVR. Interestingly, with the majority of the FEVR genes playing a role in the Wnt pathway, there could be a genetic link to the S1P vascular pathway as well.

4.5 *fzd4*$^{-/-}$ mutant zebrafish do not possess an obvious early larval phenotype

As *LRP5* and *FZD4* together are responsible for the majority (approximately 40%) of FEVR cases in humans (Toomes et al., 2005) and the most detailed retina studies in mice are from *Fzd4* mouse models (Wang et al., 2012; Wang et al., 2001; Xu et al., 2004; Ye et al., 2009), we chose to study the phenotype induced by knocking out the *Fzd4* gene in the zebrafish. Intriguingly, the *fzd4*$^{-/-}$ mutant fish did not possess an obvious phenotype at an early larval time point, rendering it not useful for preliminary drug screen. Retinal whole mounts of *fzd4*$^{-/-}$ mutant zebrafish at the one-month time point (**Figure 3.13**) displayed similarities to the phenotype previously described in the Berman Zebrafish Laboratory at three months (areas of hyper-vascularity and overall disorganization) (**Figure 1.7**) and we were interested in testing the utility of this model to study the effect of candidate drugs/compounds directly on the retina vasculature in the zebrafish. The treatment of larval *fzd4*$^{-/-}$ mutant zebrafish with 50 nM JTE-013 was chosen as this was one of the concentrations in the JTE-013 preliminary drug screen in *cdh5* morphant zebrafish found to improve early retinal vasculature. In addition, the technique of carrying out retinal whole mounts on small organisms such as zebrafish proved to be technically difficult and results from this particular experiment likely need

further, more detailed quantification analyses. The role of zebrafish at this stage is unclear and needs to be balanced with the well-established mouse models of FEVR for further testing.

One theory why the *fzd4*$^{-/-}$ mutant line did not appear to have a phenotype present in larval stages may be due to gene compensation, whereby genes compensate for other mutated genes, but this is unclear given that the phenotype does appear at later stages of development (Rossi et al., 2015). There is also little known about the pharmacokinetics of JTE-013 specifically in fish. It would be helpful to pursue pharmacokinetic studies to further guide the choices of compounds to pursue to make drug screening even more efficient. The fact that there are several stages of retina vascular development suggest that disruption may occur at any point to result in delayed vascularization of the retina and disruption of normal vascular patterning. It is clear that normal *FZD4* signaling is needed for normal vascular development. However, it is possible that the effects of loss of FZD4 signaling influence processes specific to angiogenesis and not vasculogenesis, the earlier phase of vascular development. We tried to phenotype the earlier stages of FEVR in the *fzd4*$^{-/-}$ zebrafish and although it is clear that a phenotype was present at the one-month zebrafish stage, retinal mounts on small organisms like the zebrafish are technically challenging and other techniques will be required to describe and quantify retina vascular development beyond the larval stage. To this end, we recently acquired a lightsheet microscope that will enable us to study the retina vasculature in these fish possibly eliminating the need for technically difficult flat mounts. The results of these studies may expand the utility of the FEVR zebrafish models in the development of novel therapeutics.

4.6 Potential significance for other retinal vascular disorders

Importantly, ROP is considered a major cause of blindness in children in high and middle-income countries highlighting the importance of retinal vasculature research (Holmstrom et al., 1998). Interestingly, cases of ROP have been reported where both *NDP* and *FZD4* are mutated, making the Wnt pathway a likely candidate to target for therapy (Dailey et al., 2015). It is possible that therapeutics developed to treat FEVR, including those targeting S1PR2, may also be re-purposed for ROP as there is also evidence that mutations in *FZD4* are present in some severe cases of ROP (Ells et al., 2010). Studies have linked defects in Wnt signaling to diabetes mellitus, again providing a broader justification for pursuing an orphan disease such as FEVR (Gilmour, 2015).

4.7 Limitations

Determining whether the eye size parameter "area inner eye" is clinically significant is necessary and should be further validated as more compounds are tested to see if the same parameters appear to be most affected. The data taken from the preliminary drug screens in zebrafish are only meant to guide drug discovery studies in mouse models. It would be difficult and inaccurate to make predictions regarding dosage and compound concentration in humans based on zebrafish studies.

In light of future drug screens utilizing a water bath, compound solubility is likely to be an issue. To note, DMSO and PTU are commonly used in zebrafish research and were used in the water bath in the preliminary drug screen. It is not known if adding these reagents to the water bath potentially alter the effect of the compound being screened, however DMSO is known to permeate biological membranes and therefore its

likely that the DMSO added to the water baths increased the ability of the compound to enter the zebrafish (Kais et al., 2013; Karlsson et al., 2001).

Interpretation of the *fzd4*$^{-/-}$ retinal whole mounts proved to be difficult to draw any concrete conclusions. Experiments would benefit from using a retina isolation procedure that does not damage the retina, such as lightsheet microscopy.

4.8 Future Directions

There are numerous avenues to pursue in an effort to identify novel effective therapeutics for FEVR. For instance, a qualitative vascular analysis needs to be carried out on the *cdh5* morphants which were treated with "compound 1". One would expect that if eye size is an accurate surrogate for severity of retinal vasculature, then those *cdh5* morphants in the 20 nM group should have worse retinal vasculature as well. Finally, to ensure that measuring eye size is accurately depicting retinal vasculature severity, the remaining 13 compounds should be pursued as well as taking a ligand-based approach in drug design. JTE-013 analogues can be tested using this drug screening platform in zebrafish to guide further mouse model studies.

Alternative to focusing on targeting S1PR2, future research could also focus on synthesizing compounds predicted to be S1PR1 and 3 agonists, the promoters of vascular development in this pathway. After screening a 100 000 compound library, SEW2871 was identified as a selective S1PR1 agonist (Sanna et al., 2004). S1PR2 elicits an angiostatic effect via Rac and Rho (GTPases) (**Figure 1.4**) (Park et al., 2012). Therefore, if a molecule was synthesized that could inhibit one of these GTPases, perhaps the vascular pathology would also be reversed. For example, a Rho inhibitor, C3-exotoxin,

was used to protect against renal ischemic injury and functions by inhibiting Rho (Park et al., 2012). A combination of computational software, multidisciplinary scientists, and experimental science is likely to lead to rapid drug discovery.

As an alternative to the compound water bath, one could inject JTE-013 intravenously in the common cardinal vein and subsequently grow the mutants to adulthood and analyze the retinal mounts. Intravenous compound injections are an attractive route as an alternative to the current water bath method and could be pursued with the remaining compounds (**Table 1.2**). If the compounds were injected intravenously, the amount of compound each zebrafish would have in circulation is more predictable. This method is also more analogous to the method of administration a patient is likely to receive (e.g. ocular injections).

Given the role VE-cadherin has in blood vessel integrity, it is likely that those morphants or mutants lacking this gene would show evidence of blood vessel leakage. Vessel leakiness is often diagnosed and monitored in humans using intravenous fluorescein angiography (IVFA). A fluorescent dye is injected into the patient's bloodstream and within seconds the dye will circulate its way to the retinal blood vessels at the back of the eye. From this, hyper or hypo-flourescence can be observed indicative of areas of concern (Newsome, 1986). IVFA is an invaluable tool to monitor the patient's condition. IVFA can reveal areas of avascularity, especially with wide-field FA, considering many cases of FEVR will have an avascular peripheral retina.. Dextran dye injections are a commonly used method to investigate the integrity of blood vessels in zebrafish but few studies have focused solely on retinal vasculature (Nasevicius et al., 2000; Wu et al., 2015). Therefore, it would be useful for future studies involving our

zebrafish models of FEVR to investigate retinal vessel leakage using these previously established methods as another measure of disease and whether novel treatments normalize retina vascular integrity.

It would also be interesting to investigate whether the MTD is altered in zebrafish, which have been injected with a control saline, are used in toxicity curve experiments instead of WT zebrafish unexposed to injections because mortality is generally higher in zebrafish who have undergone the injection process (preliminary studies done in Berman Zebrafish Laboratory). Laboratories that have the means to access technology such as the Biosorter (Union Biometrica), which will be coming soon to Dalhousie University, could also greatly increase drug screening efficiency and are well equipped to support zebrafish as a model organism and will be valuable to future drug discovery research. A Biosorter has the ability to sort and dispense zebrafish (and other small model organisms) into 96 well plates at a much faster rate as compared to pipetting by hand. This could expand our capacity to screen novel drugs/compounds.

Targeting other signaling pathways involved in blood vessel development is another avenue worth pursuing for therapeutic targets. Although most studies focus on the canonical Wnt signaling pathway due to its involvement in endothelial cell growth, it is possible that the non-canonical pathway may also be involved by stimulating cytoskeletal rearrangement followed by expansion of endothelium to form new vessels (Sauter et al., 2014). This was investigated with a *Cdh5* cellular model. *Cdh5* was also observed to have a role in endothelial cell shape (Nelson et al., 2004). Pursuing current and newly discovered signaling pathways, which affect blood vessel development, will aid in closing the gap of unknown genetic information about FEVR.

For example, *glycogen synthase kinase 3 beta* (*Gsk3 β*) is a negative modulator in endothelial cells and participates in the phosphoinositide-3-kinase/protein kinase B (PI3K/AKT) intracellular signaling pathway that has a known role in vessel formation during development (Lee et al., 2014; Graupera et al., 2008). S1PR1 also promotes angiogenesis via the PI3K/AKT pathway (Takuwa et al., 2001). *Gsk3 β* encodes a protein kinase, which is ubiquitously expressed in many different model organisms (eg. yeast and mammals) (Lee et al., 2014). Following knockdown of *Gsk3 β* by injecting an MO targeting *Gsk3 β* into zebrafish or by loss of *Gsk3 β* by addition of LiCl, results indicated decreased patterning of blood vessels as well as reduced vegf transcripts. The paper by Lee and colleagues (2014) suggests a cross-talk may exist between the PI3K/AKT and Wnt/β-catenin signaling pathway providing another branch of the S1P signaling pathway to pursue therapeutically.

Future studies should focus on the specificity and efficacy of the *cdh5* MO. Given that CDH5 plays a role in β-catenin levels, one could monitor the presence, absence, or levels of β-catenin to correlate this effect with gene knockdown (Wheelock & Johnson, 2003).

4.9 Conclusions

This project contributes to the visual research field by confirming that zebrafish can serve as a valuable tool to study not only the morphology of a FEVR-like phenotype, but also to study the effects of compounds suspected of reversing the pathology of this genetic condition. Compounds of interest found in this study may have potential to be used in other retinal vascular conditions such as diabetes mellitus and ROP. Results from

this research will guide the choice of S1PR2 antagonists that will move forward to further testing in mouse models and potential human clinical trials.

The idea of finding a therapeutic approach for such an orphan disease as FEVR is a highly attractive target as there is potential for drug repurposing for multiple other ocular vascular disorders, which have increased population prevalence. Overall, the results from this study leave behind a concrete platform in the zebrafish model organism for screening compounds of interest, leading the way for an exciting avenue in therapeutic drug discovery of human vascular retinal disease.

REFERENCES

Allen, R. C., Russell, S. R., Streb, L. M., Alsheikheh, a, & Stone, E. M. (2006). Phenotypic heterogeneity associated with a novel mutation (Gly112Glu) in the Norrie disease protein. *Eye (London, England)*, 20(2), 234–241. doi:10.1038/sj.eye.6701840

Alvarez, Y., Cederlund, M. L., Cottell, D. C., Bill, B. R., Ekker, S. C., Torres-Vazquez, J., … Kennedy, B. N. (2007). Genetic determinants of hyaloid and retinal vasculature in zebrafish. *BMC Developmental Biology*, 7, 114. doi:10.1186/1471-213X-7-114

Auer, T. O., & Del Bene, F. (2014). CRISPR/Cas9 and TALEN-mediated knock-in approaches in zebrafish. *Methods*, 69(2), 142–150. doi:10.1016/j.ymeth.2014.03.027

Behnia, R., & Desplan, C. (2015). Visual circuits in flies: Beginning to see the whole picture. *Current Opinion in Neurobiology*, 34, 125–132. doi:10.1016/j.conb.2015.03.010

Benson, W.E. (1995). Familial Exudative Vitreoretinopathy. *American Ophthalmological Society*, *93,* 473–521. doi:10.1016/0002-9394(69)91237-9

Bergers, G., & Song, S. (2005). The role of pericytes in blood-vessel formation and maintenance. *Neuro-Oncology*, 7(4), 452–464. doi:10.1215/S1152851705000232

Bill, B. R., Petzold, A. M., Clark, K. J., Schimmenti, L., & Ekker, S. C. (2009). A primer for morpholino use in zebrafish. *Zebrafish*, 6(1), 69–77. doi:10.1089/zeb.2008.0555

Blencowe, H., Lee, A. C. C., Cousens, S., Bahalim, A., Narwal, R., Zhong, N., … Lawn, J. E. (2013). Preterm birth-associated neurodevelopmental impairment estimates at regional and global levels for 2010. *Pediatric Research*, 74(*1*), 17–34. doi:10.1038/pr.2013.204

Brevario F., Caveda L., Corada M., Martin-Padura I., Navarro P., Golay J., …Dejana E. (1995). Functional properties of human vascular endothelial cadherin (7B4/cadherin-5), an endothelial-specific cadherin. *Arteriosclerosis, Thrombosis, & Vascular Biology,* 15(8), 1229-1239.

Canadian National Institute for the Blind. (2007). Fast facts about vision loss. Retrieved from http://cnib.ca/en/about/media/vision-loss/Pages/default.aspx

Carmeliet, P., Lampugnani, M. G., Moons, L., Breviario, F., Compernolle, V., Bono, F., … Dejana, E. (1999). Targeted deficiency or cytosolic truncation of the VE-cadherin gene in mice impairs VEGF-mediated endothelial survival and angiogenesis. *Cell*, 98(2), 147–157. doi:10.1016/S0092-8674(00)81010-7

Caveda, L., Navarro, P., Breviario, F., Corada, M., Gulino, D., … Dejana, E. (1996). Rapid Publication Inhibition of Cultured Cell Growth by Vascular Endothelial. *Society*, 98(4), 886–893.

Chen, T. C., Tsai, T. H., Shih, Y. F., Yeh, P. T., Yang, C. H., Hu, F. C., … Yang, C. M. (2010). Long-term evaluation of refractive status and optical components in eyes of children born prematurely. *Investigative Ophthalmology and Visual Science*, 51(12), 6140–6148. doi:10.1167/iovs.10-5234

Clevers, H. (2009). Eyeing Up New Wnt Pathway Players. *Cell*, 139(2), 227–229. doi:10.1016/j.cell.2009.09.027

Collin, R. W. J., Nikopoulos, K., Dona, M., Gilissen, C., Hoischen, A., Boonstra, F. N., … Cremers, F. P. M. (2013). ZNF408 is mutated in familial exudative vitreoretinopathy and is crucial for the development of zebrafish retinal vasculature. *Proceedings of the National Academy of Sciences of the United States of America*, 110(24), 9856–61. doi:10.1073/pnas.1220864110

Criswick V.G. & Scheens C.L. (1969). Familial exudative vitreoretinopathy. *American Journal of Ophthalmology,* 68(4), 578-594.

Cruz-Inigo, Y. J., Acaba, L. A., & Berrocal, M. H. (2014). Surgical management of retinal diseases: proliferative diabetic retinopathy and traction retinal detachment. *Developments in Ophthalmology*, 54, 196–203. doi:10.1159/000360467

Dailey, W., Gryc, W., Garg, P. G., & Drenser, K. (2015). Frizzled-4 Variations Associated with Retinopathy and Intrauterine Growth Retardation. *Ophthalmology*, 122(9), 1917–1923. doi:10.1016/j.ophtha.2015.05.036

Easter, S., Nicola, G., 1996. The development of vision in the zebrafish (Danio rerio). *Developmental Biology*, 180, 646–663.

Ells, A., Guernsey, D. L., Wallace, K., Zheng, B., Vincer, M., Allen, A., … Robitaille, J. M. (2010). Severe retinopathy of prematurity associated with FZD4 mutations. *Ophthalmic Genetics*, 31(1), 37–43. doi:10.3109/13816810903479834

Fledelius, H. C., & Fledelius, C. (2012). Eye size in threshold retinopathy of prematurity, based on a danish preterm infant series: Early axial eye growth, pre- and postnatal aspects. *Investigative Ophthalmology and Visual Science*, 53(7), 4177–4184. doi:10.1167/iovs.12-9516

Foley, J. E., Maeder, M. L., Pearlberg, J., Joung, J. K., Peterson, R. T., & Yeh, J.-R. J. (2009). Targeted mutagenesis in zebrafish using customized zinc-finger nucleases. *Nature Protocols*, 4(12), 1855–1867. doi:10.1038/nprot.2009.209

Gaengel, K., Niaudet, C., Hagikura, K., Siemsen, B. L., Muhl, L., Hofmann, J. J., … Betsholtz, C. (2012). The Sphingosine-1-Phosphate Receptor S1PR1 Restricts Sprouting Angiogenesis by Regulating the Interplay between VE-Cadherin and VEGFR2. *Developmental Cell*, 23(3), 587–599. doi:10.1016/j.devcel.2012.08.005

Gal, M., Levanon, E.Y., Hujeirat, Y., Khayat, M., Pe'er, J. and Shalev, S. (2014) Novel mutation in TSPAN12 leads to auto- somal recessive inheritance of congenital vitreoretinal dis- ease with intra-familial phenotypic variability. *American Journal of Medical Genetics*, 2996–3002. doi: 2910.1002/ajmg.a.36739. Epub 32014 Sep 36722.

Garner, A. & Klintworth G.K. (2008). Embryological Development of the Eye. In: Guernsey D.L., Robitaille J.M., Cameron J.D., Heathcote J.G. (Eds.). Garner & Klintworth's Pathobiology of Ocular Disease, (pp. 1099-1100). New york: Informa Health Care.

Gilmour, D. F. (2014). Familial exudative vitreoretinopathy and related retinopathies. *Eye*, 29(1), 1–14. doi:10.1038/eye.2014.70

Goldberg, M. F. (1997). Persistent fetal vasculature (PFV): an integrated interpretation of signs and symptoms associated with persistent hyperplastic primary vitreous (PHPV). *American .Journal of Ophthalmology*, 124(5), 587–626. Retrieved from http://www.ncbi.nlm.nih.gov/pubmed/9372715

Gologorsky D., Chang J.S., Hess D.J., Berroca A.M. (2013). Familial exudative vitreoretinopathy in a premature child. *Ophthalmic Surgery Lasers Imaging Retina,* 44(6), 603-605.

Gore, A. V., Monzo, K., Cha, Y. R., Pan, W., & Weinstein, B. M. (2012). Vascular Development in the Zebrafish. *Cold Spring Harbor Perspectives in Medicine*, 2(5), a006684. doi:10.1101/cshperspect.a006684

Gory-Fauré, S., Prandini, M. H., Pointu, H., Roullot, V., Pignot-Paintrand, I., Vernet, M., & Huber, P. (1999). Role of vascular endothelial-cadherin in vascular morphogenesis. *Development*, 126(10), 2093–2102.

Graupera, M., Guillermet-Guibert, J., Foukas, L. C., Phng, L.-K., Cain, R. J., Salpekar, A., … Vanhaesebroeck, B. (2008). Angiogenesis selectively requires the p110alpha isoform of PI3K to control endothelial cell migration. *Nature*, 453(7195), 662–666. doi:10.1038/nature06892

Haddad R., Font R.L., Reeser F. (1978). Persistent hyperplastic primary vitreous: a clinicopathologic study of 62 cases & review of the literature. *Survey of Ophthalmology,* 23, 123-134.

Hanson, M., Roth, C. B., Jo, E., Griffith, M. T., Scott, F. L., Reinhart, G., … Stevens, R. C. (2012). Crystal Structure of a Lipid G Protein-Coupled Receptor. *Science*, 335(6070), 851–855. doi:10.1126/science.1215904

Hartsock, A., Lee, C., Arnold, V., & Gross, J. M. (2014). In vivo analysis of hyaloid vasculature morphogenesis in zebrafish: A role for the lens in maturation and maintenance of the hyaloid. *Developmental Biology*, 394(2), 327–339. doi:10.1016/j.ydbio.2014.07.024

Hisano, Y., Inoue, A., Taimatsu, K., Ota, S., Ohga, R., Kotani, H., … Kawahara, A. (2015). Comprehensive analysis of sphingosine-1-phosphate receptor mutants during zebrafish embryogenesis. *Genes to Cells*, 20(8), 647–658. doi:10.1111/gtc.12259

Holmstrom, G., Thomassen, P., & Broberger, U. (1998). Neonatal risk factors for retinopathy of prematurity - A population-based study. *Acta Ophthalmologica Scandinavica*, 76, 204–207.

Howe, D. G., Bradford, Y. M., Conlin, T., Eagle, A. E., Fashena, D., Frazer, K., … Westerfield, M. (2013). ZFIN, the Zebrafish Model Organism Database: Increased support for mutants and transgenics. *Nucleic Acids Research*, 41(D1), 854–860. doi:10.1093/nar/gks938

Hruby, V. J. (2002). Designing peptide receptor agonists and antagonists. *Nature Reviews Drug Discovery*, 1(11), 847–858. doi:10.1038/nrd939

Hu, A., Pei, X., Ding, X., Li, J., Li, Y., Liu, F., … Lu, L. (2016). Combined Persistent Fetal Vasculature: A Classification Based on High-Resolution B-Mode Ultrasound and Color Doppler Imaging. *Ophthalmology*, 123(1), 19–25. doi:10.1016/j.ophtha.2015.09.001

Hu, H., Xiao, X., Li, S., Jia, X., Guo, X., & Zhang, Q. (2016). KIF11 mutations are a common cause of autosomal dominant familial exudative vitreoretinopathy, 278–283. doi:10.1136/bjophthalmol-2015-306878

Hughes, S., Yang, H., & Chan-Ling, T. (2000). Vascularization of the human fetal retina: Roles of vasculogenesis and angiogenesis. *Investigative Ophthalmology and Visual Science*, 41(5), 1217–1228.

Jing, L., & Zon, L. I. (2011). Zebrafish as a model for normal and malignant hematopoiesis. *Disease models & mechanisms*, 4(4), 433–8. doi:10.1242/dmm.006791

Junge, H. J., Yang, S., Burton, J. B., Paes, K., Shu, X., French, D. M., … Ye, W. (2009). TSPAN12 Regulates Retinal Vascular Development by Promoting Norrin- but Not Wnt-Induced FZD4/β-Catenin Signaling. *Cell*, 139(2), 299–311. doi:10.1016/j.cell.2009.07.048

Kais, B., Schneider, K. E., Keiter, S., Henn, K., Ackermann, C., & Braunbeck, T. (2013). DMSO modifies the permeability of the zebrafish (Danio rerio) chorion-Implications for the fish embryo test (FET). *Aquatic Toxicology*, 140-141, 229–238. doi:10.1016/j.aquatox.2013.05.022

Karlsson, J., von Hofsten, J., & Olsson, P. E. (2001). Generating transparent zebrafish: a refined method to improve detection of gene expression during embryonic development. *Marine Biotechnology (NY)*, 3(6), 522–527. doi:10.1007/s1012601-0053-4

Kennis, J. T. M., & Mathes, T. (2013). Molecular eyes : proteins that transform light into biological information. *Interface Focus 3*: 20130005. http://dx.doi.org/10.1098/rsfs.2013.0005

Kitambi, S. S., McCulloch, K. J., Peterson, R. T., & Malicki, J. J. (2009). Small molecule screen for compounds that affect vascular development in the zebrafish retina. *Mechanisms of Development,* 126(5-6), 464-477.

Kono, M., Mi, Y., Liu, Y., Sasaki, T., Allende, M. L., Wu, Y. P., … Proia, R. L. (2004). The sphingosine-1-phosphate receptors S1P1, S1P2, and S1P3 function coordinately during embryonic angiogenesis. *Journal of Biological Chemistry*, 279(28), 29367–29373. doi:10.1074/jbc.M403937200

Laine, C. M., Chung, B. D., Susic, M., Prescott, T., Semler, O., Fiskerstrand, T., … Mäkitie, O. (2011). Novel mutations affecting LRP5 splicing in patients with osteoporosis-pseudoglioma syndrome (OPPG). *European Journal of Human Genetics*, 19(8), 875–881. doi:10.1038/ejhg.2011.42

Langheinrich, U. (2003). Zebrafish: A new model on the pharmaceutical catwalk. *BioEssays*, 25(9), 904–912. doi:10.1002/bies.10326

Larson, J. D., Wadman, S. A., Chen, E., Kerley, L., Clark, K. J., Eide, M., … Essner, J. J. (2004). Expression of VE-cadherin in zebrafish embryos: A new tool to evaluate vascular development. *Developmental Dynamics*, 231(1), 204–213. doi:10.1002/dvdy.20102

Lawson N.D. & Weinstein B.M. (2002). In vivo imaging of embryonic vascular development using transgenic zebrafish. *Developmental Biology,* 248(2),307-318.

Lee, H., Lin, Y., Lai, Y., Huang, W., Hu, J., Tsai, J., & Tsai, H. (2014). Glycogen synthase kinase 3 beta in somites plays a role during the angiogenesis of zebrafish embryos, *The Federation of European Journal of Biochemistry,* 281, 4367–4383. doi:10.1111/febs.12942

Li, Z., Joseph, N. M., & Easter, S. S. (2000). The morphogenesis of the zebrafish eye, including a fate map of the optic vesicle. *Developmental Dynamics*, 218(1), 175–188.

Luhmann, U. F. O., Lin, J., Acar, N., Lammel, S., Feil, S., Grimm, C., … Berger, W. (2005). Role of the Norrie disease pseudoglioma gene in sprouting angiogenesis during development of the retinal vasculature. *Investigative Ophthalmology and Visual Science*, 46(9), 3372–3382. doi:10.1167/iovs.05-0174

Mathew, L. K., Sengupta, S., Kawakami, A., Andreasen, E. A., Lohr, C. V., Loynes, C. A., … Tanguay, R. L. (2007). Unraveling tissue regeneration pathways using chemical genetics. *Journal of Biological Chemistry*, 282(48), 35202–35210. doi:10.1074/jbc.M706640200

Muller B., Orth U., van Nouhuys C.E., Duvigneau C., Fuhrmann C., Schwinger E., … Gal A. (1994). Mapping of autosomal dominant exudative vitreoretinopathy locus (EVR1) by multipoint linkage analysis in four families. *Genomics,* 20, 317–319.

Nasevicius, a, Larson, J., & Ekker, S. C. (2000). Distinct requirements for zebrafish angiogenesis revealed by a VEGF-A morphant. *Yeast (Chichester, England)*, 17(4), 294–301.

National Coalition for Vision Health. (2011). Vision Loss in Canada 2011. Retrieved from http://www.cos-sco.ca/wpcontent/uploads/2012/09/VisionLossinCanada_e.pdf

Newsome D.A. (1986). Retinal fluorescein leakage in retinitis pigmentosa. *American Journal of Ophthalmology,* 101(3), 354-360.

Norrie G. (1927). Causes of blindness in children. *Acta Ophthalmologica,* 5, 357-386.

Miyakubo H., Hashimoto K., Miyakubo S. (1984). Retinal vascular pattern in familial exudative vitreoretinopathy. *Ophthalmology,* 91(12), 1524-1530.

Nelson C.M., Pirone D.M., Tan J.L., Chen C.S. (2004). Vascular endothelial-cadherin regulates cytoskeletal tension, cell spreading, and focal adhesions by stimulating RhoA. *Molecular Biology of the Cell,* 15, 2943-2953.

Nusslein-Volhard C. & Dahm R. (2002). *Zebrafish: a practical approach*. Retrieved from: https://books.google.ca/books?id=zS-5CKOjCIgC&pg=PA61&lpg=PA61&dq=nusslein+volhard+dahm+zebrafish+mm&source=bl&ots=mqj1u0OPbM&sig=dHGKyCx0YJpEpakdjLkMkbx7H5M&hl=en&sa=X&ved=0ahUKEwiU6vLc6_zNAhUFXB4KHezpAUAQ6AEIKjAC#v=onepage&q=nusslein%20volhard%20dahm%20zebrafish%20mm&f=false

Osada, M., Yatomi, Y., Ohmori, T., Ikeda, H., & Ozaki, Y. (2002). Enhancement of sphingosine 1-phosphate-induced migration of vascular endothelial cells and smooth muscle cells by an EDG-5 antagonist. *Biochemical & Biophysical Research Communications,* 299, 483–487.

Ouyang, L. J., Yin, Z. Q., Ke, N., Chen, X. K., Liu, Q., Fang, J., … Pi, L. H. (2015). Refractive status and optical components of premature babies with or without retinopathy of prematurity at 3-4 years old. *International Journal of Clinical and Experimental Medicine*, 8(7), 11854–11861.

Park, S. W., Kim, M., Brown, K. M., Agati, V. D. D., & Lee, H. T. (2012). Inhibition of Sphingosine 1-Phosphate Receptor 2 Protects against Renal Ischemia-Reperfusion Injury, *Journal of the American Society of Nephrology,* 46, 266–280. doi:10.1681/ASN.2011050503

Parrill, A. L., Sardar, V. M., & Yuan, H. (2004). Sphingosine 1-phosphate and lysophosphatidic acid receptors : agonist and antagonist binding and progress toward development of receptor-specific ligands, 15, 467–476. doi:10.1016/j.semcdb.2004.05.006

Pendergast, S. D., & Trese, M. T. (1998). Familial exudative vitreoretinopathy: Results of surgical management. *Ophthalmology*, 105(6), 1015–1023. doi:10.1016/S0161-6420(98)96002-X

Poulter, J. A., Ali, M., Gilmour, D. F., Rice, A., Kondo, H., Hayashi, K., … Toomes, C. (2010). Mutations in TSPAN12 Cause Autosomal-Dominant Familial Exudative Vitreoretinopathy. *American Journal of Human Genetics*, 86(2), 248–253. doi:10.1016/j.ajhg.2010.01.012

Provis, J. M. (2001). Development of the primate retinal vasculature. *Progress in Retinal and Eye Research*, 20(6), 799–821. doi:10.1016/S1350-9462(01)00012-X

Prykhozhij, S. V., Rajan, V., Gaston, D., & Berman, J. N. (2015). CRISPR multitargeter: A web tool to find common and unique CRISPR single guide RNA targets in a set of similar sequences. *PLoS ONE*, 10(3), 1–18. doi:10.1371/journal.pone.0119372

Rattner, A., Wang, Y., Zhou, Y., Williams, J., & Nathans, J. (2014). The role of the hypoxia response in shaping retinal vascular development in the absence of norrin/frizzled4 signaling. *Investigative Ophthalmology and Visual Science*, 55(12), 8614–8625. doi:10.1167/iovs.14-15693

R Core Team (2016). R: A language and environment for statistical computing. R Foundation for Statistical Computing. Vienna, Austria. ISBN 3-900051-07-0, URL http://www.R-project.org/.

Richter, M., Gottanka, J., May, C. A., Welge-Lüßen, U., Berger, W., & Lütjen-Drecoll, E. (1998). Retinal vasculature changes in Norrie disease mice. *Investigative Ophthalmology and Visual Science*, 39(12), 2450–2457.

Robitaille, J. M., Zheng, B., Wallace, K., Beis, M. J., Tatlidil, C., Yang, J., … Guernsey, D. L. (2011). The role of Frizzled-4 mutations in familial exudative vitreoretinopathy and Coats disease. *The British Journal of Ophthalmology*, 95(4), 574–579. doi:10.1136/bjo.2010.190116

Robitaille, J. M., Wallace, K., Zheng, B., Beis, M. J., Samuels, M., Hoskin-Mott, A., & Guernsey, D. L. (2009). Phenotypic overlap of familial exudative vitreoretinopathy (FEVR) with persistent fetal vasculature (PFV) caused by FZD4 mutations in two distinct pedigrees. *Ophthalmic Genetics*, 30(1), 23–30. doi:10.1080/13816810802464312

Robitaille, J. M., Gillett, R. M., LeBlanc, M. a, Gaston, D., Nightingale, M., Mackley, M. P., … Bedard, K. (2014). Phenotypic Overlap Between Familial Exudative Vitreoretinopathy and Microcephaly, Lymphedema, and Chorioretinal Dysplasia Caused by KIF11 Mutations. *JAMA Ophthalmology*, 132(12), 1–7. doi:10.1001/jamaophthalmol.2014.2814

Robitaille, J., MacDonald, M. L. E., Kaykas, A., Sheldahl, L. C., Zeisler, J., Dubé, M.-P., … Samuels, M. E. (2002). Mutant frizzled-4 disrupts retinal angiogenesis in familial exudative vitreoretinopathy. *Nature Genetics*, 32(2), 326–330. doi:10.1038/ng957

Rossi, A., Kontarakis, Z., Gerri, C., Nolte, H., Hölper, S., Krüger, M., & Stainier, D. Y. R. (2015). Genetic compensation induced by deleterious mutations but not gene knockdowns. *Nature*, 13(524), 230–3. doi:10.1038/nature14580

Saint-Geniez, M., & D'Amore, P. A. (2004). Development and pathology of the hyaloid, choroidal and retinal vasculature. *International Journal of Developmental Biology*, 48(8-9), 1045–1058. doi:10.1387/ijdb.041895ms

Sanna, M. G., Liao, J., Jo, E., Alfonso, C., Ahn, M. Y., Peterson, M. S., … Rosen, H. (2004). Sphingosine 1-Phosphate (S1P) Receptor Subtypes S1P1 and S1P3, Respectively, Regulate Lymphocyte Recirculation and Heart Rate. *Journal of Biological Chemistry*, 279(14), 13839–13848. doi:10.1074/jbc.M311743200

Sauteur, L., Krudewig, A., Herwig, L., Ehrenfeuchter, N., Lenard, A., Affolter, M., & Belting, H. G. (2014). Cdh5/VE-cadherin promotes endothelial cell interface elongation via cortical actin polymerization during angiogenic sprouting. *Cell Reports*, 9(2), 504–513. doi:10.1016/j.celrep.2014.09.024

Schindelin, J., Arganda-carreras, I., Frise, E., Kaynig, V., Longair, M., Pietzsch, T., … Cardona, A. (2012). Fiji : an open-source platform for biological-image analysis, *9*(7). doi:10.1038/nmeth.2019

Seo, S. H., Yu, Y. S., Park, S. W., Kim, J. H., Kim, H. K., Cho, S. I., … Kim, J. Y. (2015). Molecular characterization of FZD4, LRP5, and TSPAN12 in familial exudative vitreoretinopathy. *Investigative Ophthalmology and Visual Science*, 56(9), 5143–5151. doi:10.1167/iovs.14-15680

Shukla D., Singh J., Sudheer G., Soman M., John R.K., Ramasamy K., Perumalsamy N. (2003). Familial exudative vitreoretinopathy (FEVR). Clinical profile & management. *Indian Journal of Ophthalmology,* 51(4), 323-328.

Skoura, A., Sanchez, T., Claffey, K., Mandala, S. M., Proia, R. L., & Hla, T. (2007). Essential role of sphingosine 1 – phosphate receptor 2 in pathological angiogenesis of the mouse retina. *The Journal of Clinical Investigation*, 117(9), 2506–16. doi:10.1172/JCI31123DS1

Takuwa N., Du W., Kaneko E., Okamoto Y., Yoskioka K., Takuwa Y. (2011). Tumor suppressive sphingosine-1-phophate receptor-2 counteracting tumor-promoting sphingosine-1-phophate receptor-1 and sphingosine kinase 1. *American Journal of Cancer Research*, 1(4), 460–481.

Toomes, C., Bottomley, H. M., Scott, S., Mackey, D. A., Craig, J. E., Appukuttan, B., … Inglehearn, C. F. (2004). Spectrum and frequency of FZD4 mutations in familial exudative vitreoretinopathy. *Investigative Ophthalmology and Visual Science*, 45(7), 2083–2090. doi:10.1167/iovs.03-1044

Toomes C. & Downey L. (2005) (Updated 2011) Familial Exudative Vitreoretinopathy, Autosomal Dominant. In: GeneReviews®. Seattle (WA): University of Washington, Seattle. Available from: http://www.ncbi.nlm.nih.gov/books/NBK1147/

van Nouhuys, C.E. (1991). Signs, complications, & platelet aggregation in familial exudative vitreoretinopathy. *American Journal of Ophthalmology,* 111, 34-41.

Wang P., Tao L.J., Yang J.F., Tang X.R., Qi Z.Y., Tian M. and Zhang J.M. (2011). Development of ocular optical components in premature and full term in- fants. *Chinese Journal of Strabismus Pediatric Ophthalmology*. 19, 131-133,135.

Wang, Y., Huso, D., Cahill, H., Ryugo, D., & Nathans, J. (2001). Progressive cerebellar, auditory, and esophageal dysfunction caused by targeted disruption of the frizzled-4 gene. *The Journal of Neuroscience : The Official Journal of the Society for Neuroscience*, 21(13), 4761–4771. doi:21/13/4761

Warburg M. (1966). Norrie's disease. A congenital progressive oculo-acoustic-cerebral degeneration. *Acta Ophthalmologica,* 89, 1-47.

Warden, S. M., Andreoli, C. M., & Mukai, S. (2007). The Wnt signaling pathway in familial exudative vitreoretinopathy and Norrie disease. *Seminars in Ophthalmology*, *22*, 211–217. doi:10.1080/08820530701745124

Westerfield, M. (2000). *The zebrafish book. A guide for the laboratory use of zebrafish (Danio rerio).* (4th ed.). Eugene: Univ. of Oregon Press.

Wise G.N., Dollery C.T., Henhind P. (1971). *The Retinal Circulation*. Harper and Row: New York.

Wheelock, M. J., & Johnson, K. R. (2003). Cadherins as modulators of cellular phenotype. *Annual Review of Cell and Developmental Biology*, 19(1), 207–235. doi:10.1146/annurev.cellbio.19.011102.111135

Williams, C. H., & Hong, C. C. (2011). Multi-Step usage of in Vivo models during rational drug design and discovery. *International Journal of Molecular Sciences*, 12(4), 2262–2274. doi:10.3390/ijms12042262

Won Park, S., Kim, M., Brown, K. M., D'Agati, V. D., & Lee, H. T. (2012). Inhibition of Sphingosine 1-Phosphate Receptor 2 Protects against Renal Ischemia-Reperfusion Injury. *Journal of the American Society of Nephrology*, 23, 266–280. doi:10.1681/ASN.2011050503

Wu, Y. C., Chang, C. Y., Kao, A., Hsi, B., Lee, S. H., Chen, Y. H., & Wang, I. J. (2015). Hypoxia-induced retinal neovascularization in zebrafish embryos: A potential model of retinopathy of prematurity. *PLoS ONE*, 10(5), 1–17. doi:10.1371/journal.pone.0126750

Xia, C., Yablonka-reuveni, Z., & Gong, X. (2010). LRP5 Is Required for Vascular Development in Deeper Layers of the Retina, *PLoS ONE* 5(7), 1–7. doi:10.1371/journal.pone.0011676

Xu, Q., Wang, Y., Dabdoub, A., Smallwood, P. M., Williams, J., Woods, C., … Nathans, J. (2004). Vascular development in the retina and inner ear: Control by Norrin and Frizzled-4, a high-affinity ligand-receptor pair. *Cell*, 116(6), 883–895. doi:10.1016/S0092-8674(04)00216-8

Yang, C. S., Wang, A. G., Shih, Y. F., & Hsu, W. M. (2013). Long-term biometric optic components of diode laser-treated threshold retinopathy of prematurity at 9 years of age. *Acta Ophthalmologica*, 91(4), 276–283. doi:10.1111/aos.12053

Ye, X., Wang, Y., Cahill, H., Yu, M., Badea, T. C., Smallwood, P. M., & Peachey, N. S. (2009). in Endothelial Cells Controls a Genetic Program for Retinal Vascularization. *Cell*, 139(2), 285–298. doi:10.1016/j.cell.2009.07.047

Yu, P. B., Hong, C. C., Sachidanandan, C., Babitt, J. L., Deng, D. Y., Hoyng, S. A., … Peterson, R. T. (2008). Dorsomorphin inhibits BMP signals required for embryogenesis and iron metabolism. *Nature Chemical Biology*, 4(1), 33–41. doi:10.1038/nchembio.2007.54

Zon, L. I. (1999). Zebrafish ：A New Model for Human Disease. *Genome research*, 9, 99–100. doi:10.1101/gr.9.2.99

Zon, L. I. & Peterson, R. T. (2005). In vivo drug discovery in the zebrafish. *Nature Reviews Drug Discovery, 4,* 35-44.

APPENDIX A COPYRIGHT AND PERMISSIONS- *PROGRESS IN RETINAL EYE RESEARCH* (ELSEVIER)

ELSEVIER LICENSE
TERMS AND CONDITIONS

Aug 28, 2016

This Agreement between Tenille Fleischhacker ("You") and Elsevier ("Elsevier") consists of your license details and the terms and conditions provided by Elsevier and Copyright Clearance Center.

License Number	3919510063143
License date	Jul 31, 2016
Licensed Content Publisher	Elsevier
Licensed Content Publication	Progress in Retinal and Eye Research
Licensed Content Title	Development of the Primate Retinal Vasculature
Licensed Content Author	Jan M. Provis
Licensed Content Date	November 2001
Licensed Content Volume Number	20
Licensed Content Issue Number	6
Licensed Content Pages	23
Start Page	799
End Page	821
Type of Use	reuse in a thesis/dissertation
Portion	figures/tables/illustrations
Number of figures/tables/illustrations	1
Format	both print and electronic

APPENDIX B COPYRIGHT AND PERMISSIONS- *OPHTHALMIC GENETICS* (TAYLOR AND FRANCIS)

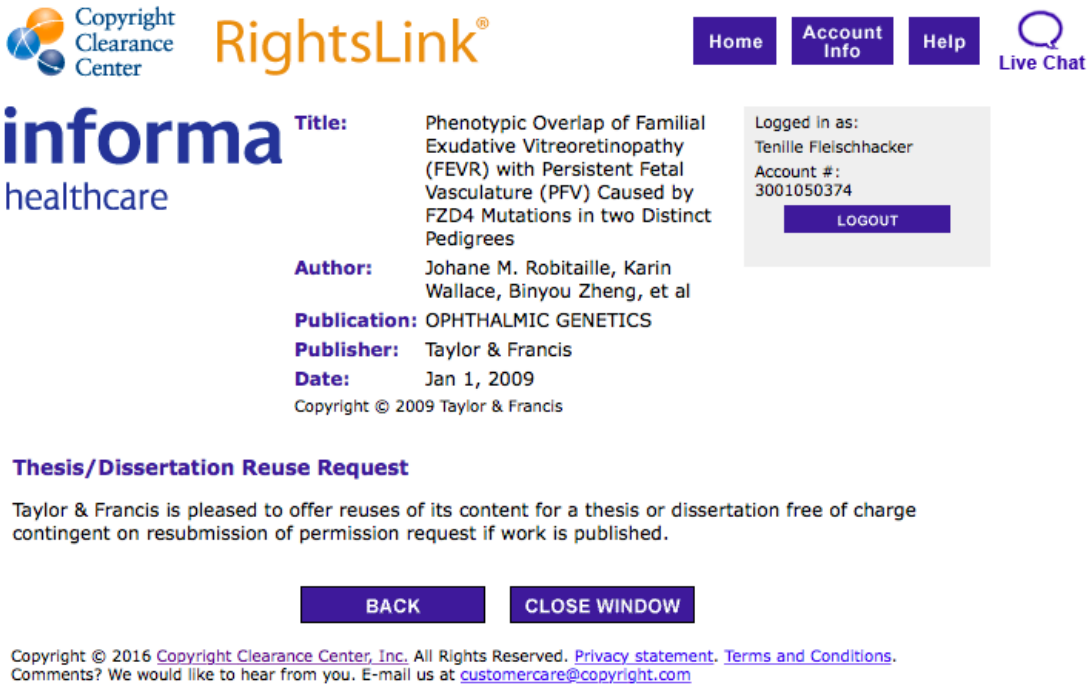

Copyright Clearance Center RightsLink®

Home | Account Info | Help | Live Chat

informa healthcare

Title: Phenotypic Overlap of Familial Exudative Vitreoretinopathy (FEVR) with Persistent Fetal Vasculature (PFV) Caused by FZD4 Mutations in two Distinct Pedigrees

Author: Johane M. Robitaille, Karin Wallace, Binyou Zheng, et al

Publication: OPHTHALMIC GENETICS

Publisher: Taylor & Francis

Date: Jan 1, 2009

Copyright © 2009 Taylor & Francis

Logged in as:
Tenille Fleischhacker
Account #:
3001050374
LOGOUT

Thesis/Dissertation Reuse Request

Taylor & Francis is pleased to offer reuses of its content for a thesis or dissertation free of charge contingent on resubmission of permission request if work is published.

BACK | CLOSE WINDOW

Copyright © 2016 Copyright Clearance Center, Inc. All Rights Reserved. Privacy statement. Terms and Conditions.
Comments? We would like to hear from you. E-mail us at customercare@copyright.com

APPENDIX C COPYRIGHT AND PERMISSIONS- *INVESTIGATIVE OPHTHALMOLOGY AND VISUAL SCIENCE* (ASSOCIATION FOR RESEARCH IN VISION AND OPHTHALMOLOGY*)*

Association for Research in Vision and Ophthalmology LICENSE TERMS AND CONDITIONS

Aug 28, 2016

This is a License Agreement between Tenille Fleischhacker ("You") and Association for Research in Vision and Ophthalmology ("Association for Research in Vision and Ophthalmology") provided by Copyright Clearance Center ("CCC"). The license consists of your order details, the terms and conditions provided by Association for Research in Vision and Ophthalmology, and the payment terms and conditions.

All payments must be made in full to CCC. For payment instructions, please see information listed at the bottom of this form.

License Number	3920241022605
License date	Aug 01, 2016
Licensed content publisher	Association for Research in Vision and Ophthalmology
Licensed content title	Investigative ophthalmology
Licensed content date	Jan 1, 1977
Type of Use	Thesis/Dissertation
Requestor type	Author of requested content
Format	Electronic
Portion	image/photo
Number of images/photos requested	1
Title or numeric reference of the portion(s)	Figure 1 c
Title of the article or chapter the portion is from	Spectrum and Frequency of FZD4 Mutations in Familial Exudative Vitreoretinopathy
Editor of portion(s)	N/A
Author of portion(s)	N/A
Volume of serial or monograph.	N/A
Page range of the portion	3
Publication date of portion	2004
Rights for	Main product

APPENDIX D COPYRIGHT AND PERMISSIONS- *CELL* (ELSEVIER)

Association for Research in Vision and Ophthalmology LICENSE TERMS AND CONDITIONS

Aug 28, 2016

This is a License Agreement between Tenille Fleischhacker ("You") and Association for Research in Vision and Ophthalmology ("Association for Research in Vision and Ophthalmology") provided by Copyright Clearance Center ("CCC"). The license consists of your order details, the terms and conditions provided by Association for Research in Vision and Ophthalmology, and the payment terms and conditions.

All payments must be made in full to CCC. For payment instructions, please see information listed at the bottom of this form.

License Number	3920241022605
License date	Aug 01, 2016
Licensed content publisher	Association for Research in Vision and Ophthalmology
Licensed content title	Investigative ophthalmology
Licensed content date	Jan 1, 1977
Type of Use	Thesis/Dissertation
Requestor type	Author of requested content
Format	Electronic
Portion	image/photo
Number of images/photos requested	1
Title or numeric reference of the portion(s)	Figure 1 c
Title of the article or chapter the portion is from	Spectrum and Frequency of FZD4 Mutations in Familial Exudative Vitreoretinopathy
Editor of portion(s)	N/A
Author of portion(s)	N/A
Volume of serial or monograph.	N/A
Page range of the portion	3
Publication date of portion	2004
Rights for	Main product

APPENDIX E COPYRIGHT AND PERMISSIONS- *AMERICAN JOURNAL OF CANCER RESEARCH* (E-CENTURY PUBLISHING CORPORTATION)

Copyright Policy

By submitting a manuscript to AJND, all authors agree that all copyrights of all materials included in the submitted manuscript will be exclusively transferred to the publisher - e-Century Publishing Corporation once the manuscript is accepted.

Once the paper is published, the copyright will be released by the publisher under the "Creative Commons Attribution Noncommercial License", enabling the unrestricted non-commercial use, distribution, and reproduction of the published article in any medium, provided that the original work is properly cited. If the manuscript contains a figure or table reproduced from a book or another journal article, the authors should obtain permission from the copyright holder before submitting the manuscript, and be fully responsible for any legal and/or financial consequences if such permissions are not obtained.

All PDF, XML and html files for all articles published in this journal are the property of the publisher, e-Century Publishing Corporation (www.e-Century.org). Authors and readers are granted the right to freely use these files for all academic purposes. By publishing paper in this journal, the authors grant the permanent right to the publisher to use any articles published in this journal without any restriction including, but not limited to academic and/or commercial purposes. If you are interested in using PDF, html, XML files or any art works published in this journal for any commercial purposes, please contact the publisher at business@e-century.org.

APPENDIX F COPYRIGHT AND PERMISSIONS- *DEVELOPMENTAL DYNAMICS* (JOHN WILEY AND SONS)

JOHN WILEY AND SONS LICENSE TERMS AND CONDITIONS

Aug 29, 2016

This Agreement between Tenille Fleischhacker ("You") and John Wiley and Sons ("John Wiley and Sons") consists of your license details and the terms and conditions provided by John Wiley and Sons and Copyright Clearance Center.

License Number	3932290552051
License date	Aug 19, 2016
Licensed Content Publisher	John Wiley and Sons
Licensed Content Publication	Developmental Dynamics
Licensed Content Title	The morphogenesis of the zebrafish eye, including a fate map of the optic vesicle
Licensed Content Author	Zheng Li,Nancy M. Joseph,Stephen S. Easter
Licensed Content Date	May 18, 2000
Licensed Content Pages	14
Type of use	Dissertation/Thesis
Requestor type	University/Academic
Format	Electronic
Portion	Figure/table
Number of figures/tables	1
Original Wiley figure/table number(s)	Figure 1 E
Will you be translating?	No
Title of your thesis / dissertation	Utilizing zebrafish to model the childhood blinding disorder, familial exudative vitreoretinopathy (FEVR), and discover novel therapeutics

APPENDIX G- ETHICS APPROVAL

DALHOUSIE UNIVERSITY
Inspiring Minds

NOTICE OF PROTOCOL APPROVAL
UNIVERSITY COMMITTEE ON LABORATORY ANIMALS

Protocol Number:	**15-134**
Previous protocol #:	**13-130**
Principal Investigator:	**Dr. Jason Berman**
Expiry Date:	**December 1, 2016**
Title of Study:	**Zebrafish as a Model to Study Rare and Orphan Diseases**
Species:	**Fish**

Jennifer Wipp
UCLA@dal.ca
University Committee on Laboratory Animals
902-494-1270
WEBSITE: http://www.dal.ca/dept/animal-ethics.html

In compliance with granting agency and Dalhousie University policy, Dalhousie Research Services is not permitted to release funding instalments into research accounts until documentation of all necessary approvals are submitted (i.e. Human ethics, animal ethics, biohazard and radiation permits).